

# NOAA 11 Solar Backscatter Ultraviolet, model 2 (SBUV/2) instrument solar spectral irradiance measurements in 1989-1994

## 2. Results, validation, and comparisons

Matthew T. DeLand and Richard P. Cebula

Raytheon STX Corporation, Lanham, Maryland

**Abstract.** Accurately measuring long-term solar UV variability is an experimental challenge because instrument response degradations are typically large enough to obscure solar change. For satellite instruments, one solution is a series of regular comparisons with a well-calibrated reference. The NOAA 11 Solar Backscatter Ultraviolet, model 2 (SBUV/2) instrument made solar spectral irradiance measurements between 170 and 400 nm from December 1988 to October 1994, covering the maximum and most of the decline of solar cycle 22. The NOAA 11 irradiance data were corrected for long-term instrument sensitivity changes using comparisons with coincident flights of the Shuttle SBUV (SSBUV) instrument. The NOAA 11 data show a decrease of  $7.0(\pm 1.8)\%$  in smoothed 200-208 nm irradiance from Cycle 22 maximum in mid-1989 to October 1994, near solar minimum. The long-term decrease in solar irradiance at 250 nm was  $\sim 3.5(\pm 1.8)\%$ . Longward of 300 nm, no solar variations were observed to within the 1% accuracy of the data. The NOAA 11 measurements overlap observations from the Upper Atmosphere Research Satellite (UARS) Solar Stellar Irradiance Comparison Experiment (SOLSTICE) and Solar Ultraviolet Spectral Irradiance Monitor (SUSIM) instruments from October 1991 to October 1994, providing the first opportunity to compare three coincident long-term solar UV irradiance data sets. We find reasonable agreement between the NOAA 11, SOLSTICE, and SUSIM results at all wavelengths in the 170-400 nm region. Power spectral analysis gives consistent results for all three instruments on solar rotational timescales, and reveals the evolution of solar rotation periodicity and strength during a solar cycle. We find significant differences between instruments in both period and spectral location when the spectral irradiance data are analyzed on intermediate (50-250 days) timescales. The NOAA 11 spectral irradiance data provide a valuable complement to the UARS solar data, and capture the entire maximum of solar cycle 22.

## 1. Introduction

Characterization of solar activity is a key aspect of a comprehensive understanding of the Earth's climate, both past and present. Variations in the visual appearance of the Sun have been observed for  $\sim 2000$  years and quantified in the form of sunspot numbers since the 17th century [Foukal, 1990]. During the first half of the 20th century, many observers attempted to determine whether the integrated, or "total," solar irradiance  $S$  varied over short (days to weeks) or long (months to years) time scales (see Hoyt [1979] for a review of the Smithsonian Astrophysical Observatory program). Although some observers claimed to see variations of 1-2% on short timescales, long-term variations were difficult to reliably extract. Hoyt [1979] has reanalyzed the Smithsonian data and found  $\Delta S \leq 0.1\%$  over 30 years. The advent of satellite-based total irradiance measurements in the late 1970s and early 1980s provided much more precise data. Current estimates of  $\Delta S$  are  $\sim 0.10$ - $0.15\%$  over an 11-year solar cycle, with short-term decreases up to 0.2% due to large sunspot groups (see the review by Lean [1991]).

While the solar irradiance in the visible wavelength region ( $\sim 400$ - $700$  nm) is nearly constant, the nature of solar activity changes in the middle and near ultraviolet (UV) region, defined here as  $\sim 200$ - $400$  nm. For  $\lambda \approx 300$ - $400$  nm, the emitted solar radiation is basically photospheric, with the exception of deep absorption features such as Ca II  $K$  and  $H$  at 393.4 and 396.8 nm, whose cores are generated in the lower chromosphere. Long-term variations at these wavelengths are believed to be  $< 1\%$  over a solar cycle, which is below current capabilities for direct irradiance measurements. In the region  $\sim 180$ - $300$  nm, observed solar radiation is generated in the upper photosphere. Variations on both short and long timescales are observed, which can be correlated with solar magnetic activity. The amplitude of the variability increases at shorter wavelengths. The short-term variations are caused by bright active regions (plages and faculae) rotating in and out of the field of view as seen from Earth, giving a nominal period of 27 days corresponding to the solar rotational period [Lean, 1987]. The decay of old regions and emergence of new regions (possibly at different heliocentric longitudes) during all periods of moderate to high solar activity leads to variations of  $\pm 3$  days in the observed solar rotational period over time. Irradiance variations on timescales of several months are also produced by this growth/decay process but are rarely periodic in nature. Long-term variations tend to follow the level of magnetic activity, with contributions from

Copyright 1998 by the American Geophysical Union.

Paper number 98JD01204.  
0148-0227/98/98JD-01204\$09.00

active network components as well as plagues [Harvey and Livingston, 1994].

## 2. Measurement History

Measurements of solar irradiance from the Earth's surface are only capable of measuring meaningful irradiance values down to ~295 nm. The determination of the absolute solar irradiance and its variability in the mid-UV therefore requires the use of rockets, balloons, and/or satellites to gather the necessary data. Rocket instruments have the advantage that absolute calibrations can be obtained both before and after flight, but they can only provide a "snapshot" in time of solar behavior. The first solar measurements in the mid-UV wavelength region were made from a V-2 rocket in 1946 [Baum *et al.*, 1946]. Further measurements in the 1950s and early 1960s were reviewed by Tousey [1963], and additional measurements were obtained in the late 1960s and mid-1970s by various groups and individuals [e.g., Broadfoot, 1972; Heroux and Swirbalus, 1976]. In the 1980s, multiple rocket experiments were flown by groups at the University of Colorado/Laboratory for Atmospheric and Space Physics [Mount and Rottman, 1981, 1983a, b] and NASA Goddard Space Flight Center [Mentall *et al.*, 1981, 1985; Mentall and Williams, 1988]. Solar UV irradiance measurements in the 200-300 nm region have also been made from stratospheric balloons [e.g., Hall, 1983; Hall and Anderson, 1984]. The calibration accuracies of these measurements have generally been insufficient to permit quantitative estimates of solar variability, although Hall [1983] noted a 20% increase from solar cycle minimum to maximum in the emission cores of the Mg II *h* and *k* lines at 279.6 and 280.3 nm.

Satellite instruments offer the best method to determine the magnitude of solar UV variability on rotational and solar cycle timescales through the accumulation of extended time series. The first such instruments designed to measure mid-UV solar activity were launched in the 1968-1970 period. A photodiode experiment measuring in the 30-210 nm region was flown on an Air Force satellite in July 1968 [Prag and Morse, 1970], with a 27-day lifetime. The Monitor of Ultraviolet Solar Experiment (MUSE) instrument also used broadband photodiodes centered at 120, 180, and 260 nm for flights on the Nimbus 3 (April 1969 to January 1972) [Heath, 1969] and Nimbus 4 (April 1970 to May 1977) spacecraft, as well as an August 1966 rocket flight [Heath, 1973]. In addition, the Backscattered Ultraviolet (BUV) spectrometer, measuring at 12 discrete wavelengths between 255 and 340 nm, was also flown on Nimbus 4. These instruments gave the first quantitative estimates of solar UV variability on rotational timescales, ranging from 60% at 115-210 nm [Prag and Morse, 1970] to ~4% at 200 nm and 1% at 300 nm [Heath, 1973]. Hinteregger [1976] examined data from the solar EUV spectrometer (EUVS) instrument on the AE-C satellite and found rotational modulation of  $\leq 15\%$  in the 135-185 nm region between January 1974 and May 1975. These limited long-term observations did identify a serious difficulty with satellite UV measurement instruments, specifically the rapid degradation rate of instrument optics. For Nimbus 3 MUSE, an exponential decay in signal strength was observed, with changes up to 25% over a single orbit during severe geomagnetic conditions [Heath, 1973]. The aluminum diffuser plate used to provide a diffuse source of solar irradiance for the Nimbus 4 BUV instrument was also found to rapidly decrease in reflectivity (a factor of 2-3 at 255 nm in less than 6 months (D. F. Heath, unpublished data, 1975)) due to continuous exposure, such that a meaningful estimate of long-term solar UV irradiance variability could not be determined [Flieger *et al.*, 1981]. These large instrument response changes were a major impediment to the characterization of long-

term solar UV variability. The review by Smith and Gottlieb [1974] concluded that there was no variability in the solar irradiance longward of 150 nm over a solar cycle. Ackerman [1974] suggested that while there might be solar cycle irradiance variations of a few percent at  $\lambda < 210$  nm, it was unlikely that corresponding effects would be observable in stratospheric ozone. However, in sharp contrast to those conclusions, the MUSE and BUV data were combined to infer much larger variations on solar cycle timescales, ~80% at 200 nm and 18% at 300 nm [Heath and Thekaekara, 1977]. A review by Simon [1981] proposed considerably lower values for solar cycle variability ( $\Delta F = 10$ -20% at 175-200 nm, < 10% at 200-240 nm, < 2% at 240-330 nm) but also noted that the long-term repeatability of available data was only ~10%.

The next set of significant satellite solar spectral UV measurements began near the maximum of solar cycle 21, with the launch of the Nimbus 7 Solar Backscatter Ultraviolet (SBUV) instrument in October 1978. The primary objective of the SBUV instrument was the measurement of stratospheric ozone profiles using back-scattered UV radiation [Heath *et al.*, 1975]. Nimbus 7 SBUV also made daily spectral solar UV measurements in the wavelength region 160-400 nm at 1.1-nm resolution from November 1978 to February 1987 by deploying a diffuser plate to direct sunlight into the nadir-viewing instrument. Although the SBUV instrument did not carry an onboard calibration system, changes in the frequency of observations during its operational lifetime were used to assess long-term instrument sensitivity changes [Cebula *et al.*, 1988; Herman *et al.*, 1990; Schlesinger and Cebula, 1992]. Using data corrected by this method, estimated solar irradiance changes from maximum to minimum for cycle 21 (incorporating all error estimates) were 5-8% at 205 nm and 1-4% at 210-260 nm [Schlesinger and Cebula, 1992]. Daily solar spectral UV data were also taken from January 1982 to April 1989 by the Solar Mesosphere Explorer (SME) satellite [Rottman *et al.*, 1982; Rottman, 1988]. SME made solar measurements over the 120-300 nm wavelength region at 0.75-nm resolution, using a single Ebert-Fastie spectrometer. Long-term instrument response changes were characterized by comparing the primary "working" solar diffuser with a seldom-used test diffuser, which was assumed to be stable over time. Absolute calibration was determined from several rocket observations [e.g., Mount and Rottman, 1983a]. The estimated error in the long-term drift correction was ~2%/yr at Lyman  $\alpha$  (121.6 nm) and ~1%/yr at 200-300 nm [Rottman, 1988]. Thus the estimated solar irradiance variations measured by SME for the decline of cycle 21 were ~50( $\pm 10$ )% at 121.6 nm (Ly  $\alpha$ ), 6( $\pm 4$ )% at 200 nm, and 2( $\pm 4$ )% at 300 nm. The solar cycle variation results from Nimbus 7 SBUV and SME are in general agreement within their respective  $\pm 1\sigma$  error bars. However, the magnitude of the uncertainty in these solar variability measurements, roughly 3-4%, is still large relative to the accuracy desired.

Solar irradiance in the 200-300 nm wavelength region is largely absorbed in the stratosphere, where it directly impacts ozone abundances through the modification of photolysis rates. Theoretical work predicts [e.g., Brasseur, 1993; Fleming *et al.*, 1995; Jackman *et al.*, 1996] and observations confirm [e.g., Chandra and McPeters, 1994; Keating *et al.*, 1994; Reinsel *et al.*, 1994; Callis *et al.*, 1997] an approximate 1.2-2.0% solar cycle-driven variation of global mean total ozone. Solar cycle variations in stratospheric temperature and geopotential height are also observed [e.g., McCormack and Hood, 1996; Hood, 1997]. These solar cycle length ozone changes are comparable to the observed ~2%/decade long-term decrease in total ozone [Bojkov *et al.*, 1995]. Thus tracking long-term solar change to an accuracy of ~1% near 205 nm is required to thoroughly understand the role of solar variations in atmospheric change (L. Hood, private communication, 1997). For

solar cycle 22, numerous additional satellite data sets are available to help quantify long-term solar UV spectral variability.

### 2.1. SBUV/2 Instruments

The NOAA 9 SBUV/2 instrument [Frederick *et al.*, 1986] began taking spectral scan solar measurements in March 1985 and continued near daily observations until May 6, 1997. These data constitute the longest set of solar UV measurements from a single instrument. These measurements are very similar to the Nimbus 7 SBUV measurements, covering the 160–400 nm wavelength region at 1.1-nm resolution. Discrete solar measurements at 12 wavelengths surrounding the Mg II absorption line at 280 nm began in May 1986 and continued through February 1998. NOAA 9 spacecraft operations were terminated on February 19, 1998. The SBUV/2 discrete solar data provide better signal-to-noise and wavelength stability than the spectral scan data, but only 12 wavelengths are observed. NOAA 9 discrete Mg II index data have been published by Donnelly *et al.* [1994] and DeLand and Cebula [1998]. NOAA 9 was designed with an onboard calibration system to monitor diffuser plate changes during flight, but the system did not operate correctly [Frederick *et al.*, 1994], and calibrated irradiance data are not currently available. Cebula *et al.* [1992] and DeLand and Cebula [1993] constructed a Mg II proxy index from the NOAA 9 spectral scan irradiance data to study both short-term and long-term solar UV variability. The uncorrected spectral scan data can also provide information on short-term variability [Schlesinger *et al.*, 1990; DeLand and Cebula, 1998]. The NOAA 11 SBUV/2 instrument, which also carried an onboard calibration system, was launched in September 1988 and began taking data in December 1988. NOAA 11 solar measurements continued until the failure of the diffuser mechanism in October 1994. The onboard calibration system worked well for this instrument [Weiss *et al.*, 1991; Hilsenrath *et al.*, 1995] and characterized the long-term changes in diffuser reflectivity to an accuracy of  $\pm 0.2\%/yr$  ( $2\sigma$ ). Remaining instrument throughput changes observed in solar measurements could not be characterized solely from onboard data and required an alternative method of characterization. Comparisons with coincident measurements from the Shuttle SBUV (SSBUV) instrument were used to derive corrected NOAA 11 irradiances, as discussed by Cebula *et al.* [this issue]. The NOAA 14 SBUV/2 instrument was launched in December 1994 and commenced regular solar observations in February 1995. This instrument began experiencing grating drive problems during spectral scan observations in July 1995, and by September 1995 the spectral scan data were no longer usable shortward of 280 nm. NOAA 14 spectral scan solar measurements were terminated on October 6, 1995.

### 2.2. Other Satellite Instruments

The Airglow-Solar Spectrometer Instrument (ASSI) flew on the San Marco 5 satellite between March 25 and December 6, 1988. It used 18 overlapping channels to cover the wavelength range 20–700 nm, with a resolution of  $\sim 1$ –3 nm [Schmidtke *et al.*, 1983]. A reference EUV spectrum has been published for comparison with coincident rocket and SME spectral data [Schmidtke *et al.*, 1992], but the full data set is not yet available. Beginning in September 1991, two instruments onboard the Upper Atmosphere Research Satellite (UARS) have provided daily solar spectral UV irradiance data: Solar Stellar Irradiance Comparison Experiment (SOLSTICE) [Rottman *et al.*, 1993; Woods *et al.*, 1993] and Solar Ultraviolet Spectral Irradiance Monitor (SUSIM) [Brueckner *et al.*, 1993]. SOLSTICE has a resolution of  $\Delta\lambda \approx 0.1$ –0.2 nm for daily measure-

ments, while SUSIM uses resolutions of 1.1 nm and 5 nm for daily measurements and  $\Delta\lambda \approx 0.15$  nm for weekly measurements. Both of these instruments have greater wavelength coverage ( $\sim 115$ –410 nm) than the SBUV/2 instruments, and each contains an onboard calibration system capable of monitoring end-to-end sensor response changes. The Global Ozone Monitoring Experiment (GOME) instrument on the Earth Remote Sensing (ERS-2) platform is a double monochromator employing four 1024-element diode arrays to cover the wavelength range 240–790 nm, with a resolution of  $\Delta\lambda \approx 0.2$  nm in the mid-UV [Peeters *et al.*, 1996]. It has been making measurements since its launch in May 1995 and began daily observations in June 1996 [Weber *et al.*, 1998]. The Solar Oscillations and Variability (SOVA) experiment flew on the European Recoverable Carrier (EURECA) recoverable satellite from August 10, 1992 to May 16, 1993 [Wehrli *et al.*, 1995], using three 5 nm photometers centered at 335, 500, and 862 nm. Sensitivity changes in the 335-nm photometer were very rapid (50% during the first 7 days of operation) due to the high duty cycle [Wehrli *et al.*, 1996]. This experiment was designed to look at short-term variations (timescales of minutes to days), so long-term response changes were not deemed to be critical.

### 2.3. Shuttle Experiments

The space shuttle provides an alternative approach to the determination of long-term solar change, allowing instruments to take measurements during individual flights separated by months or years. Extensive preflight, inflight, and postflight calibration are used to achieve the desired accuracy in lieu of continuous observations. Shuttle-based solar irradiance measurements began with the Solar Spectrum (SOLSPEC) instrument in December 1983 [Labs *et al.*, 1987] and continued with the shuttle SUSIM instrument in August 1985 [VanHoosier *et al.*, 1988] and the SSBUV instrument in 1989, 1990, 1991, 1994, and 1996 [Cebula and Hilsenrath, 1992; Cebula *et al.*, 1994]. These three instruments also flew together on the ATLAS missions in 1992, 1993, and 1994 [Cebula *et al.*, 1996, 1998; Woods *et al.*, 1996; Thullier *et al.*, 1997].

Although the SBUV/2 instruments do not have end-to-end calibration monitoring, the NOAA 11 data have been corrected for throughput change using comparisons with coincident SSBUV data [Cebula *et al.*, this issue]. The procedures discussed by Cebula *et al.* [this issue] give absolutely calibrated solar UV data from the NOAA 11 SBUV/2 instrument covering December 1988 to October 1994. Section 3 presents an analysis of the NOAA 11 SBUV/2 irradiance data set, discussing both temporal and spectral variations of the data, and showing comparisons of observed solar activity variations with proxy index predictions. Next, we present comparisons with contemporaneous UARS SUSIM and SOLSTICE data from October 1991 to September 1994 to evaluate the consistency of solar UV irradiance variations determined from three different instruments on two separate satellite platforms during the latter half of solar cycle 22. Section 6 examines the nature of periodic solar activity during cycle 22 using periodogram analysis, with discussion of both temporal and spectral characteristics.

## 3. NOAA 11 Irradiance Data

A complete description of the NOAA 11 SBUV/2 instrument and its normal measurement program are given by Cebula *et al.* [this issue] (hereinafter referred to as paper 1). NOAA 11 began making solar irradiance measurements on December 2, 1988, and made daily solar spectral irradiance measurements from February 14, 1989, to October 19, 1994. Each daily measurement consisted of two scans over the 160–406 nm wavelength region at 1.1-nm

resolution and approximate 0.15-nm sampling. Earth view and solar view science data and in-flight calibration data were used to derive corrections for long-term changes in features of the instrument characterization such as goniometry, interrange ratio, and wavelength scale drift. An onboard calibration system used a mercury lamp to monitor long-term changes in diffuser plate reflectivity and wavelength calibration. Additional discussion of these steps is given by paper 1 and *Hilsenrath et al.* [1995]. Because the SBUV/2 instruments do not have the capability to internally monitor end-to-end calibration changes, an external reference source was needed to characterize the remaining instrument response changes in the NOAA 11 irradiance data. This was accomplished through comparisons with coincident measurements by the SSBUV instrument [*Hilsenrath et al.*, 1988; *Cebula et al.*, 1994]. Full details of this procedure are presented in paper 1. All NOAA 11 SBUV/2 data are unavailable for the month of March 1991. As described in paper 1, additional data gaps are present in September-December 1993, January-April 1994, and August-September 1994 due to shadowing caused by the drifting satellite orbit.

The NOAA 11 solar spectral irradiance data are available as daily spectra with 1.1-nm resolution over the wavelength range 170-400 nm; data taken at  $\lambda < 170$  nm were found to be too noisy for useful analysis, and the NOAA 11 prelaunch calibration is only valid to 400 nm. A typical spectrum is shown in Figure 1 at the instrument sampling of  $\Delta\lambda \approx 0.15$  nm. Prominent features include the Al ionization edge at 208 nm, the Mg ionization edge at 251 nm, Fe II absorption lines at 260 and 263 nm, the unresolved Mg II absorption feature at 280 nm, the Mg I absorption line at 285 nm, and the Ca II K and H absorption lines at 393.4 and 396.8 nm. For ease of comparison with archived results from the UARS instruments, the NOAA 11 data are presented in this paper as 1 nm averages on 0.5-nm centers. This provides improved signal-to-noise (SNR) for NOAA 11, with six to seven samples averaged for each 1-nm bin. The accuracy of the averaged data may have a slight dependence on spectral location, since the wavelength drift correction procedure used in paper 1 may not perfectly represent all changes in regions with sharp irradiance changes, such as the Mg I ionization edge (251 nm) or the Mg II absorption feature (280 nm).

In order to evaluate the quality and information contained in the NOAA 11 solar irradiance data, it is convenient to first consider broad spectral regions. The wavelength region 300-400 nm can be considered to represent the lower photosphere. At the moderate SBUV/2 resolution of  $\Delta\lambda = 1.1$  nm, most of the absorption lines in this region are not resolved (excepting major features such as Ca II K and H), so that the observed irradiance approximates the photospheric continuum. Figure 2a shows the time series of a representative 10 nm band in this wavelength region (330-340 nm). The overall change in irradiance is  $< 1\%$  from February 1989 to October 1994. These irradiances were normalized to the average of February 15-17, 1989, because that period represents the start of regular NOAA 11 daily operations, whereas the December 1988 and January 1989 data were taken only occasionally during in-flight instrument activation and evaluation operations. Long-term solar variations are believed to be  $< 1\%$  for  $\lambda > 300$  nm [*Lean*, 1991; *DeLand and Cebula*, 1993; *Chandra et al.*, 1995], so the trend in Figure 2a probably indicates the long-term accuracy of the corrected irradiance data. The rise during 1989 suggests a possible overcorrection for instrument response changes. However, as discussed in paper 1, the limited temporal sampling available from SSBUV coincidences and the noise level of the NOAA 11 data makes it difficult to refine the characterization of instrument change without making an a priori assumption as to the final time dependence of the irradiance data. The magnitude and temporal dependence of the long-term variation in Figure 2a is generally representative of all NOAA 11 data in the 300-400 nm region.

Observed solar irradiance data in the 265-300 nm wavelength region are lower than the values predicted from the  $\sim 5700$  K blackbody temperature that approximates the solar irradiance at longer wavelengths. While light at these wavelengths is expected to show little solar variability because it originates relatively low in the photosphere, the presence of deep absorption features such as Mg II and Mg I and the rapid absolute irradiance change (a factor of 6-8 over  $\Delta\lambda = 30$  nm) can complicate the analysis for large wavelength bands. A time series plot averaged over 265-275 nm looks very similar to the 300-400 nm data through mid-1992 but shows additional fluctuations in late 1992 and 1993 (Figure 2b). Analysis of narrow bands reveals that this change is predominately

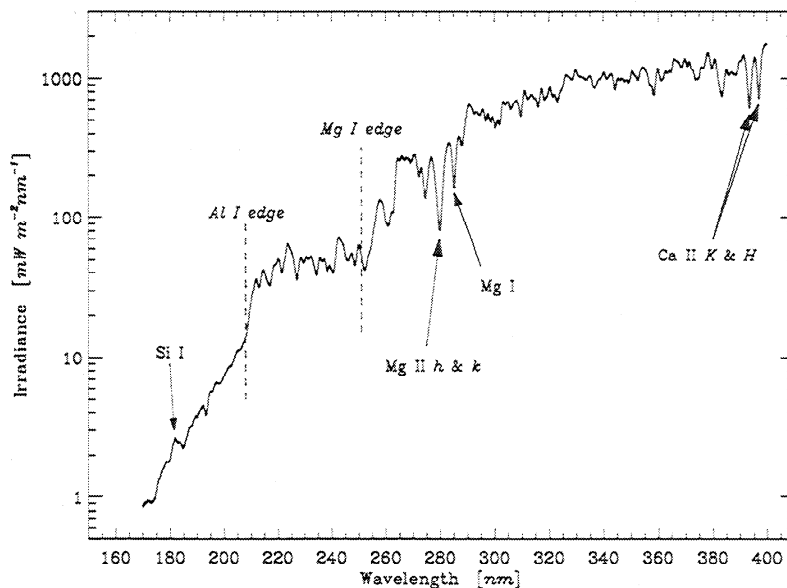
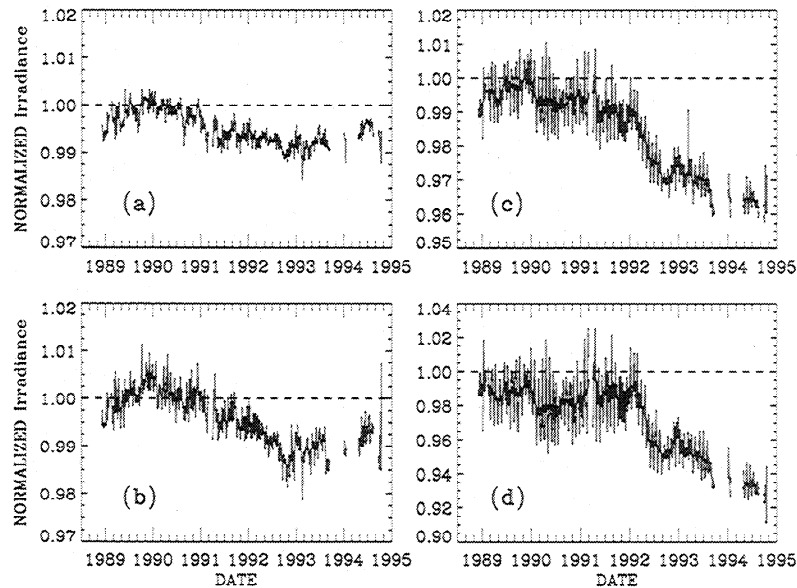


Figure 1. The solar irradiance spectrum as measured by NOAA 11 SBUV/2 on December 5, 1988, showing the location of significant spectral features.



**Figure 2.** NOAA 11 irradiance time series averaged over (a) 330-340 nm, (b) 265-275 nm, (c) 240-250 nm, and (d) 200-208 nm. Each time series has been normalized to the average of February 15-17, 1989. A 5-day binomial average has been applied for clarity. The heavy line in Figures 2c and 2d represents a 27-day running average of the data.

caused by wavelength regions which encompass rapid irradiance changes, such as 268-272 nm. Note that the 265-300 nm region is somewhat problematic for NOAA 11 irradiance measurements because the SBUV/2 instrument's electronic design forces a gain range change at  $F_{abs} \approx 150-175 \text{ mW m}^{-2}\text{nm}^{-1}$ , so that measurements in this region may have relatively poor SNR levels. Data taken at lower or higher irradiance values have significantly better SNR levels.

The wavelength region 210-260 nm is shortward of the strong Fe II absorption features at 260 and 263 nm and provides the first large-scale example of rotational and long-term solar activity. The NOAA 11 irradiance data averaged over 240-250 nm are representative of this wavelength region, and the time series plot in Figure 2c shows rotational modulation of up to 3% peak-to-peak (p-p) during 1989 and 1991. Using a 27-day running average to remove the effects of rotational activity indicates long-term solar decrease in this spectral region of 2.5-3.0% from late 1989 through the end of the NOAA 11 data record in October 1994. Based on sunspot number,  $R_z$ , Wilson [1995] suggests that the maximum of cycle 22 was reached in July 1989, with a secondary maximum in 1991. We find significant peaks with comparable strength in fall 1989, spring 1991, and spring 1992 in the smoothed irradiance data, which makes it difficult to unambiguously define the "maximum" of cycle 22. A sharp drop in solar activity during spring 1992 can be also seen in Figure 2c, which is associated with the decrease in southern hemisphere magnetic flux as discussed by White *et al.* [1994]. The 170-208 nm wavelength region is shortward of the Al ionization edge and is the primary driver for stratospheric photochemistry. Aside from a few relatively weak emission lines (e.g., Si II at 181.6 nm), these irradiances are generated in the upper photosphere. A time series plot of the irradiance averaged over 200-208 nm is representative of the increased solar activity in this wavelength region (Figure 2d), and shows approximately twice as much activity as the 210-260 nm region, with up to 6-7% rotational modulation during solar maximum, and a long-term decrease of ~6% from early 1992 through late 1994.

In order to get an overall sense of the long-term solar spectral irradiance variations measured by the NOAA 11 SBUV/2 instru-

ment without making dozens of repetitive time series plots, we have combined time series results such as Figure 2 to produce the spectral change results shown in Plate 1. Plate 1 is composed of 10-nm bands over the full 170-400 nm wavelength range observed by NOAA 11. The NOAA 11 long-term calibration in the 170-200 nm region used a self-correcting method because coincident SSBUV measurements were unavailable, as described in paper 1. Since these data have a greater long-term uncertainty than the rest of the NOAA 11 irradiance data, the dashed line in Plate 1 identifies the transition between the two regions. Data points exceeding  $\pm 5\sigma$  from the time series average in each wavelength band were screened before plotting. Each time series was smoothed with an 81-day running average to remove solar rotational activity, then averaged in 10-day bins to improve temporal clarity and normalized to the bin representing the start of regular NOAA 11 SBUV/2 operations (February 10-19, 1989). Vertical black stripes represent periods where no NOAA 11 data are available. The NOAA 11 irradiance data show no "long-term" solar changes greater than  $\pm 1\%$  (light blue, light green) for most data longward of ~270 nm and for the 210-270 nm region during 1989-1991. The long-term changes in the level of solar activity at the Al ionization edge (~210 nm) and the Mg ionization edge (~250 nm) are easily identified in Plate 1. The end of the solar cycle 22 maximum in spring 1992 is also prominent, with an amplitude of approximately -1.5% between March 1992 and July 1992 over the 210-250 nm region and approximately -4% between 170 and 210 nm during the same interval.

A significant challenge with the NOAA 11 solar irradiance data is deciding how to determine the accuracy of the instrument throughput correction. The long-term relative accuracy derived in paper 1 ranges from  $\pm 0.9\%$  ( $2\sigma$ ) at ~350-400 nm to  $\pm 2.3\%$  ( $2\sigma$ ) at 180 nm. We would like to achieve the accuracy observed at long wavelengths, i.e.,  $\pm 1\%$  over 5.5 years, for the entire 170-400 nm spectral region in order to satisfy the requirements discussed earlier for stratospheric change. However, the presence of significant solar activity at wavelengths shortward of 265 nm complicates the evaluation of the NOAA 11 irradiance data in this region. As described by DeLand and Cebula [1993], an independent estimate

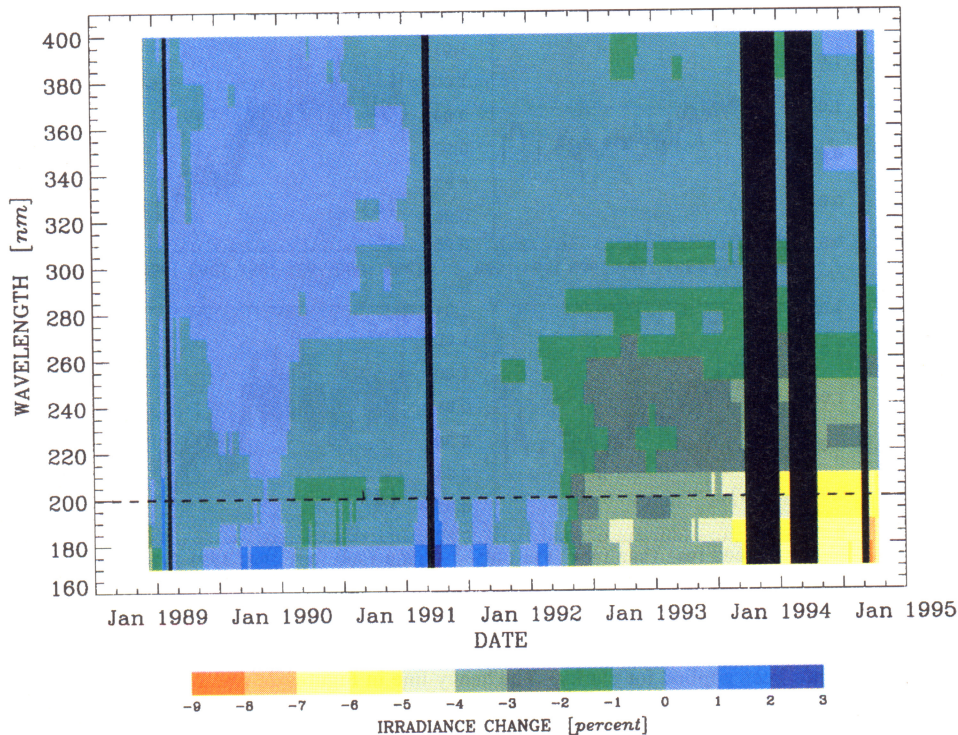


**Plate 1.** NOAA 11 spectral irradiance change between December 1988 and October 1994, shown as percent change from February 10 to 19, 1989. An 81-day running average has been applied. Data are averaged in 10-nm, 10-day bins. The dashed line identifies a change in long-term calibration technique, as discussed in the text.

of solar spectral irradiance variations can be derived using the Mg II index and scale factors. The Mg II index uses measurements of the Mg II absorption line at 280 nm to derive an index of chromospheric activity which is insensitive to instrument throughput changes [Heath and Schlesinger, 1986]. In this paper, we use the NOAA 11 "classical discrete" Mg II index presented by Cebula and DeLand [1998] and shown in Figure 3a. The NOAA 11 Mg II index shows rotational modulation of up to 7% during 1989-1991 and a long-term change (27-day smoothed) of  $\sim 7.5\%$  between 1989 and 1994.

The scale factor values shown in Figure 3b were developed from analysis of solar rotational variations [DeLand and Cebula, 1993]. The irradiance changes predicted by the chromospheric Mg II index and scale factors could be incorrect if  $\Delta \text{Mg II}(t)$  does not accurately represent  $\Delta F(\lambda, t)$  on long time scales. Kariyappa and Sivaraman [1994] found network elements to represent  $\sim 25\%$  of the disc-averaged Ca II K line emission from spectroheliograms taken between 1957 and 1983 and showed the network contribution to be anticorrelated with large-scale solar activity during solar cycles 19-21. However, Harvey and Livingston [1994] used full-disk images at He I (10830 Å) to show that the increase of  $\sim 35$  mÅ in the equivalent width of that line (excluding rotational modulation) from solar minimum in 1986 to maximum in 1989-1991 comes from 10 mÅ background, 15-20 mÅ plages, and 5-10 mÅ filaments. The overall shape of the long-term response is the same for all three components despite the differences in amplitude, which implies that the scale factor method yields appropriate results for both short and long timescales. Chandra et al. [1995] derived scale factors from UARS SOLSTICE and SUSIM irradiance data in the 120-200 nm wavelength region and the Mg II index data of Donnelly et al. [1994] over both short and long timescales. They found the same scale factor values for the 200-205 nm region in both cases but

suggested that scale factors based on rotational modulations underpredict long-term irradiance variations for wavelengths shortward of 175 nm. For wavelengths longward of 300 nm, irradiance enhancements due to plages and filaments are in competition with irradiance decreases caused by sunspot darkening. Any resulting net irradiance variations are difficult to separate from instrumental effects. Lean et al. [1997] use a two component irradiance model incorporating both facular brightening (via the Mg II index) and a sunspot darkening function to more effectively represent solar UV variability in this spectral region. The Mg II proxy model predicts no solar change at the  $\pm 1\sigma$  level between 290 and 400 nm, with the exception of absorption lines such as Fe I (385 nm) and Ca II (393.4, 396.8 nm).

Using the NOAA 11 Mg II index and scale factors, we have estimated the solar changes at 200-208 nm and 240-250 nm during 1989-1994. The average scale factor from DeLand and Cebula [1993] is  $1.05(\pm 0.02)$  at 200-208 nm and  $0.45(\pm 0.05)$  at 240-250 nm, so that the predicted solar changes are approximately  $-7.9\%$  and  $-3.2\%$ , respectively. These changes are consistent with the values of 7% at 200-205 nm and 3% at 250-255 nm predicted by Lean et al. [1992] using a similar technique. Both predictions are in good agreement with the NOAA 11 observations, which indicate a 27-day averaged change of  $7.0(\pm 1.8)\%$  at 200-208 nm and  $\sim 3.5(\pm 1.8)\%$  at 250 nm. If the observed solar signal  $S$  is represented by  $S = IR$ , where  $I$  is the solar irradiance and  $R$  is the instrument response, then the estimated solar changes calculated by the scale factor model allow us to evaluate the drift in  $R$  with time. The desolarized data ( $R = S/I$ ) at 240-250 nm, shown in Figure 4a, exhibit a drift of less than 1% during 1989-1994. Figure 4b shows that the desolarized data at 200-208 nm varies by  $\sim 1\%$  during the 5.5-year NOAA 11 data record, with some additional drift occurring during initial operations in December 1988 and January 1989.

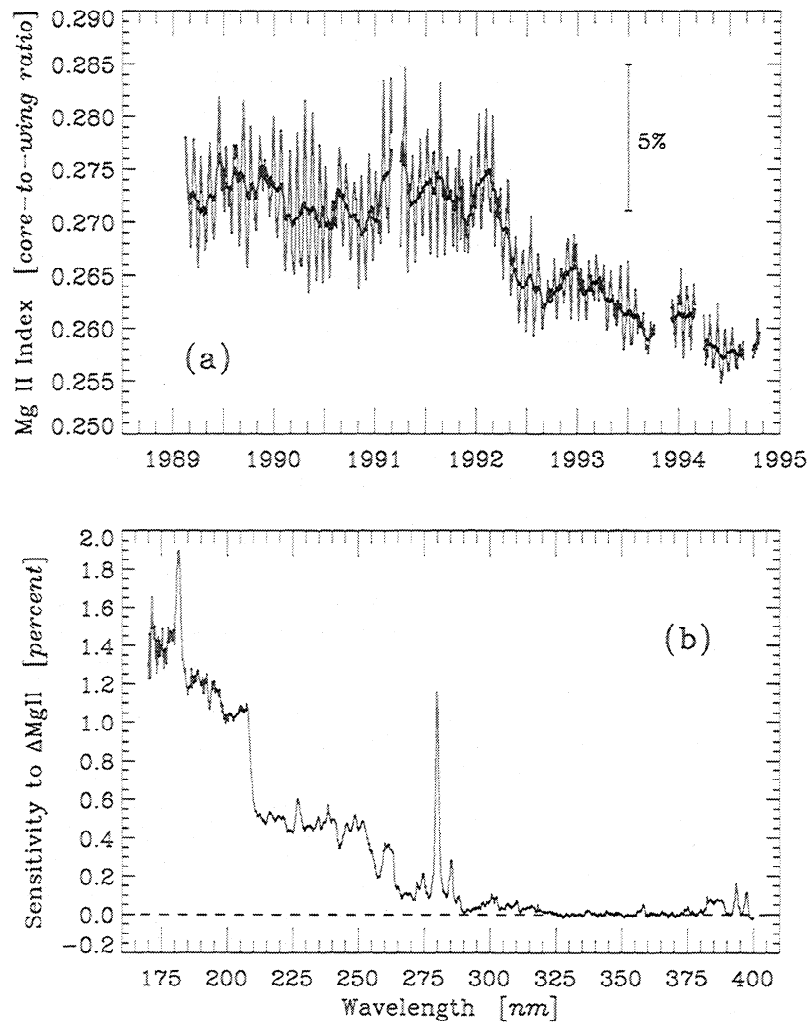


Figure 3. (a) Time series of the NOAA 11 "classical discrete" Mg II index [from *Cebula and DeLand, 1998*]. The heavy line represents a 27-day running average of the data. (b) Scale factors for irradiance change [from *DeLand and Cebula, 1993*].

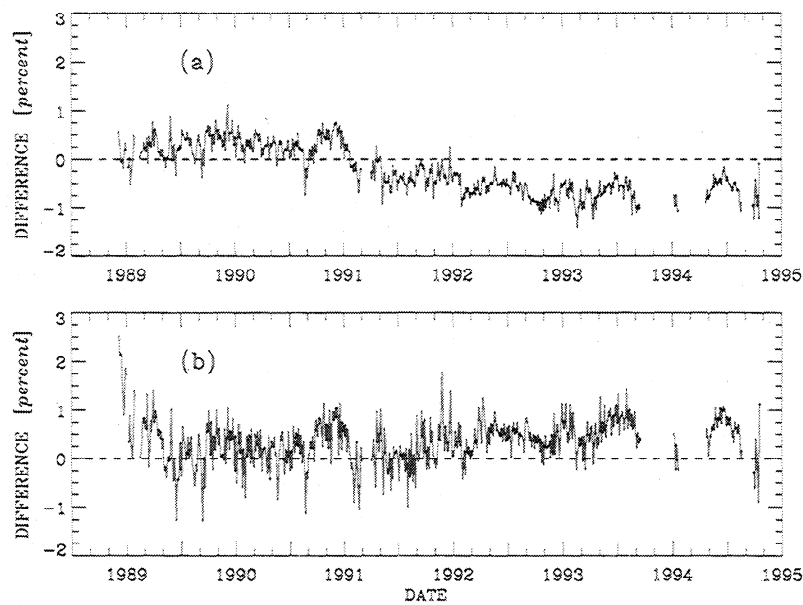


Figure 4. (a) NOAA 11 irradiance time series at 240-250 nm, "desolarized" by removing predicted solar change. A 5-day binomial average has been applied for clarity. (b) NOAA 11 desolarized irradiance time series at 200-208 nm.

These results suggest that any residual errors in the NOAA 11 SBUV/2 instrument response corrections are basically wavelength-independent down to 210 nm or so, with some additional error (1-2%) at shorter wavelengths.

We would like to know how to apportion the remaining differences in Figure 4 between the NOAA 11 instrument response correction and the proxy model prediction. The NOAA 11 "classical discrete" Mg II index was compared with the NOAA 9 classical discrete Mg II index and the UARS SOLSTICE and SUSIM Mg II indexes by *Cebula and DeLand* [1998]. They found that the NOAA 11 Mg II data drifted by <1% relative to the NOAA 9 Mg II data during 1989-1994 and were also stable to within 1% relative to the SUSIM Mg II data (after an initial drift, that seems to be in the SUSIM data). This suggests that the error in the long-term solar variation predicted by the NOAA 11 Mg II index is approximately 1% or less. Thus the actual decrease in the 200-208 nm irradiance based on NOAA 11 measurements is 6-7% from 1989 to 1994.

The composite scale factors from *DeLand and Cebula* [1993] shown in Figure 3b are predominantly influenced by the *Heath and Schlesinger* [1986] Nimbus 7 SBUV results. The NOAA 9 and NOAA 11 scale factors had larger uncertainties, and thus we can ask whether those results can be improved. Rederiving the NOAA 11 scale factors with the corrected NOAA 11 irradiance data would probably not have a major effect, since most of the corrections presented in paper 1 were primarily aimed at long-term behavior.

A more significant impact would come from using the cleaner classical discrete Mg II data, as well as additional rotations, to better constrain the calculated scale factors. We plan to address these issues in the future. For this paper, we can now compare the NOAA 11 SBUV/2 data with solar irradiance data from other instruments.

#### 4. UARS Solar Data

The UARS satellite, launched in September 1991, carries a suite of instruments designed to provide a comprehensive study of the upper atmosphere and the influences upon it [*Reber*, 1990]. UARS has two instruments dedicated to solar UV measurements. SUSIM has a tandem spectrometer design, and covers the wavelength range 115-410 nm with daily measurements at 1.1-nm resolution [*Brueckner et al.*, 1993], using onboard calibration lamps to track long-term calibration changes [*Floyd et al.*, 1996; *Prinz et al.*, 1996]. SOLSTICE measures solar irradiances over a similar wavelength range (115-420 nm) but has a different spectrometer design [*Rottman et al.*, 1993] and observes an ensemble of blue-white stars for long-term calibration purposes [*Woods et al.*, 1993; *Rottman and Woods*, 1994]. In this paper, we use the SUSIM V19 irradiance data, which are available for the period October 1991 to September 1996. The V19 data are very similar to the V18 irradiance data described by *Floyd et al.* [1998], which end in January 1996. The SOLSTICE data used here are the V09 product from the Goddard Space Flight Center Distributed Active Archive Centre (GSFC DAAC), which cover the period October 1991 through December 1996. The pointing accuracy of the UARS solar instrument platform was relatively poor during the first few months of operation (September-November 1991) [*Woods et al.*, 1996], causing fluctuations in the SOLSTICE and SUSIM irradiance data which are believed to be instrumental in origin (G. De Toma and O. R. White, private communication, 1997). We have excluded SOLSTICE and SUSIM data taken prior to November 28, 1991, from the comparisons presented in this paper.

Comparison of absolute irradiances between different satellite instruments can be problematic. Use of the first operational, or "day 1," data minimizes the effects of postlaunch calibration changes, but one must account for possibly less stable initial

behavior as well as different solar activity conditions between the dates of interest. If simultaneous measurements are used, the accuracy of corrections for different instrument histories becomes important. In Figure 5, we compare the NOAA 11 irradiance measurements with the average of four other solar spectral UV measurements (UARS SUSIM, UARS SOLSTICE, ATLAS SUSIM, and ATLAS SOLSPEC) taken on March 29, 1992, coincident with the ATLAS 1 shuttle mission. This is ~6 months after the start of UARS SUSIM and SOLSTICE observations and ~3 years into the NOAA 11 data record. The behavior of the two UARS instruments at this time is well documented in the UARS validation paper by *Woods et al.* [1996]. A detailed comparison of the ATLAS 1 SUSIM, SOLSPEC, and SSBUV shuttle-based solar irradiance measurements is given by *Cebula et al.* [1996]. We constructed the average of UARS SUSIM, UARS SOLSTICE, ATLAS SUSIM, and ATLAS SOLSPEC irradiance data over the 170-400 nm wavelength region for March 29, 1992, as an external reference spectrum which is independent of the NOAA 11 SBUV/2 data. Figure 5 shows that NOAA 11 has a spectral bias relative to the ATLAS 1 average spectrum, ranging from -3% at 220 nm to +8% at 360 nm. These results are broadly consistent with the absolute irradiance comparison between the NOAA 11 "day 1" spectrum and the flight-averaged data from SSBUV 2 in October 1990, shown in Figure 5 of paper 1. Periodic spectral structure with a length of ~60 nm is also present longward of ~260 nm. As discussed in paper 1, *Fowler* [1994] has shown the presence of similar structure in the ratio of SBUV/2 radiometric calibrations performed in air and vacuum. The NOAA 11 uncertainty budget presented in Table 3 of paper 1 shows that the irradiance difference in Figure 5 is within the NOAA 11  $\pm 2\sigma$  absolute uncertainty between 180 and 350 nm but exceeds that range at wavelengths greater than 350 nm. Shortward of ~190 nm, the NOAA 11 SBUV/2 sensitivity rapidly decreases with decreasing wavelength, concurrent with diminishing laboratory irradiance standard intensity. The combination of these effects acts to increase the uncertainty in the NOAA 11 calibration and likely contributes the majority of the irradiance difference shown in that spectral region. The decreased sensitivity leads to greater uncertainty in NOAA 11 data shortward of 200 nm, as shown in Table 3 of paper 1. We recommend the use of SSBUV or UARS solar irradiance data if an absolute accuracy of better than 5% is required.

#### 5. Time Series Comparisons

To facilitate comparisons between NOAA 11 SBUV/2, UARS SUSIM, and UARS SOLSTICE, the remainder of this paper will focus on the concurrent measurement period December 1991 to September 1994. All irradiance time series shown here are normalized to the value for December 1, 1991, for each band and instrument, and all points exceeding  $\pm 5\sigma$  limits are removed. A 5-day binomial-weighted average was used to smooth spikes in the time series without excessively dampening true solar variations. As mentioned in section 3, solar irradiance time series at wavelengths longward of 300 nm should offer a good indication of residual errors in the instrument characterization due to the lack of significant solar activity. Figure 6 shows that for all three instruments, the 1991-1994 data at 330-340 nm are consistent with long-term solar change not exceeding 1%. Observed long-term variations are within the  $\pm 1\%$  uncertainty predicted for each instrument. This level of agreement is generally present for most 10-nm bands longward of the Fe II absorption feature at 260-263 nm. The NOAA 11 data are slightly noisier than SUSIM and SOLSTICE, with occasional spikes up to 1% in the band-averaged time series caused by single 1-nm wavelength bins.

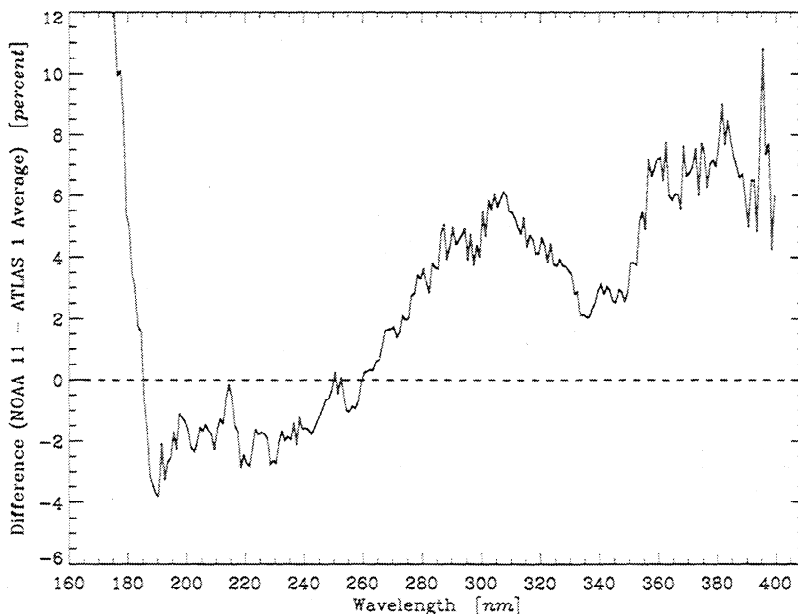


Figure 5. NOAA 11 SBUV/2 spectral irradiance difference relative to the average of UARS SUSIM, UARS SOLSTICE, ATLAS-1 SUSIM, and ATLAS-1 SOLSPEC for March 29, 1992. Both spectra were smoothed with a 5 nm average.

For shorter wavelengths, where solar activity becomes significant, all three instruments show similar representations of solar behavior. The time series at 240-250 nm in Figure 7 show 1.0-1.5% rotational modulation during 1991-1994 and an overall decline of ~3%. Individual "spikes" for a given instrument (e.g., March 1993 for NOAA 11, March 1994 for SUSIM, September 1993 for SOLSTICE) are easily identified as anomalous data. In other cases, such as September 1992 for NOAA 11 and August

1994 for SOLSTICE, reduced or absent rotational modulation becomes apparent only when compared with contemporaneous data from other instruments. The irradiance data for the 200-208 nm region shown in Figure 8 also look fairly consistent between these three instruments, with a long-term decrease of approximately -6% from early 1992 to mid-1994, persistent 27-day rotational modulation of ~2-3%, and an interval of approximate 13-day periodicity in early 1993.

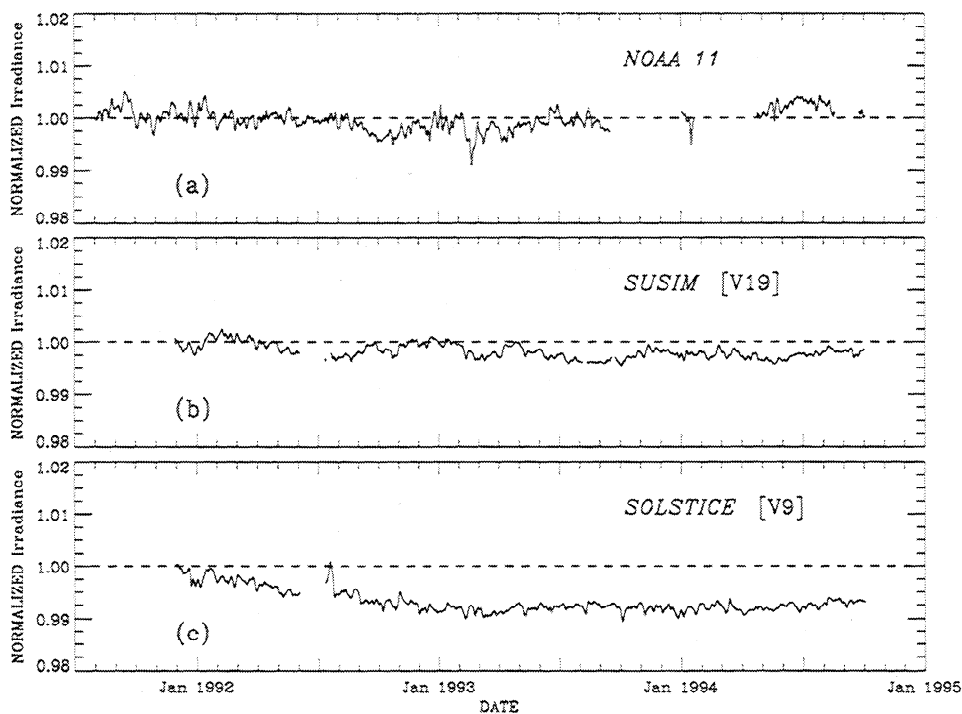
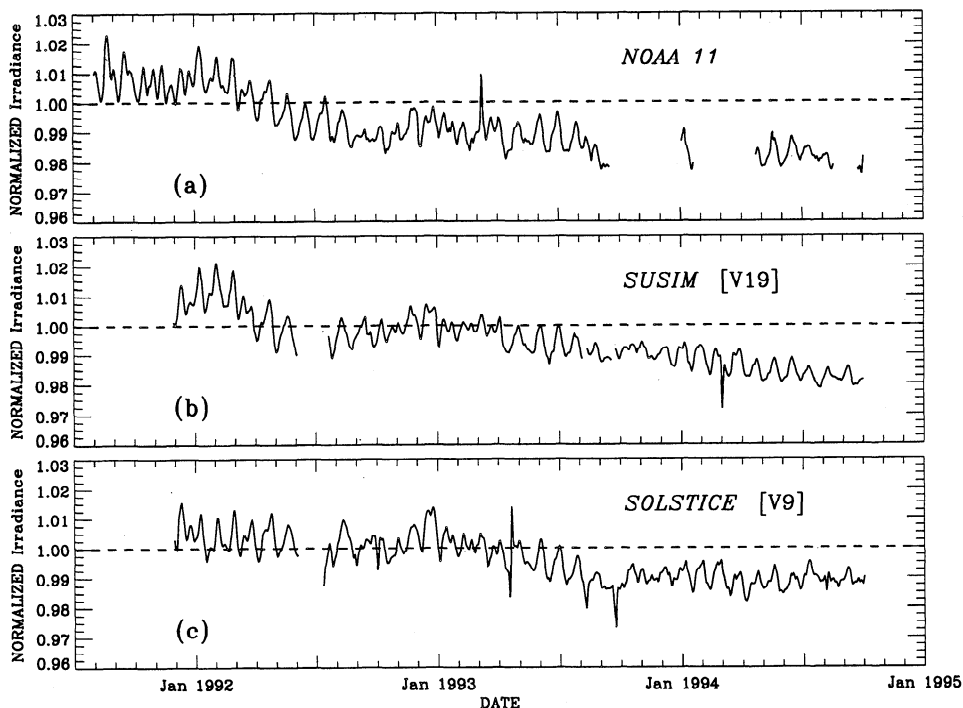


Figure 6. Solar irradiance time series at 330-340 nm: (a) NOAA 11, (b) SUSIM, and (c) SOLSTICE. All time series have been normalized to December 1, 1991, and smoothed with a 5-day binomial average.



**Figure 7.** Solar irradiance time series at 240-250 nm: (a) NOAA 11, (b) SUSIM, and (c) SOLSTICE. All time series have been smoothed with a 5-day binomial average.

As a test of the degree to which each instrument is able to monitor the varying amplitude of solar rotational modulation and long-term activity changes, we remove the modeled solar irradiance changes from each data set using the NOAA 11 Mg II index and scale factors prediction described earlier. This method simplifies the comparison of instrument behavior because it avoids the problem

of determining the origin of a relative drift inherent to the use of ratios between instruments. The desolarized time series at 240-250 nm in Figure 9 shows that NOAA 11 and SUSIM data are in good agreement with the predicted solar variations, with differences in the  $\pm 0.5\%$  range. The SOLSTICE data vary by  $\pm 1\%$  during the first half of 1992 (Figure 9c), which is consistent with the predicted

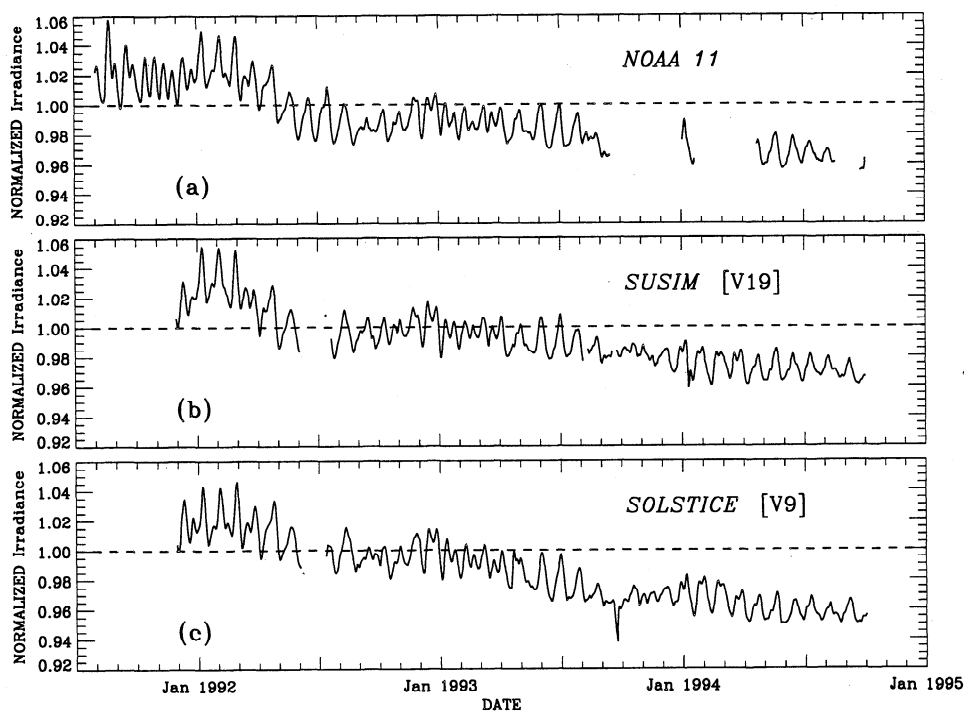


**Figure 8.** Solar irradiance time series at 200-208 nm: (a) NOAA 11, (b) SUSIM, and (c) SOLSTICE. All time series have been smoothed with a 5-day binomial average.

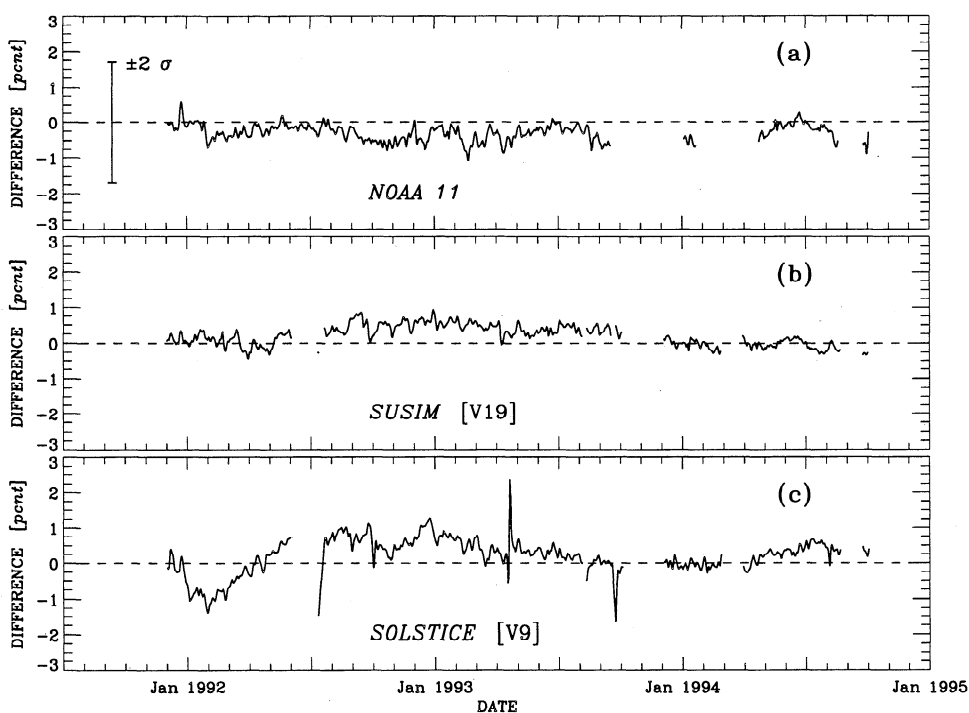


**Figure 9.** Desolarized irradiance time series at 240-250 nm: (a) NOAA 11, (b) SUSIM, and (c) SOLSTICE. All time series have been smoothed with a 5-day binomial average. The  $\pm 2\sigma$  uncertainty in Figure 9a is taken from *Cebula et al.* [this issue].

uncertainty. The long-term change in the desolarized data at 200-208 nm shown in Figure 10 for each instrument is  $\pm 1\%$  or less in October 1994 relative to December 1991. The SUSIM data fluctuate  $\sim 2\%$  in late 1993 relative to the other instruments (Figure 10b), while SOLSTICE data increase by 2% during the first half of 1992 before decreasing over the next few months (Figure 10c). The

fluctuations observed for the UARS instruments do not exceed the  $\pm 2\sigma$  uncertainty derived for the NOAA 11 data in paper 1. All three data sets in Figure 10 show suggestions of residual short-term periodic behavior at the 0.5-1.0% level, particularly during the interval of 13-day periodicity in early 1993. This result, which suggests that during periods of significant 13-day periodicity the

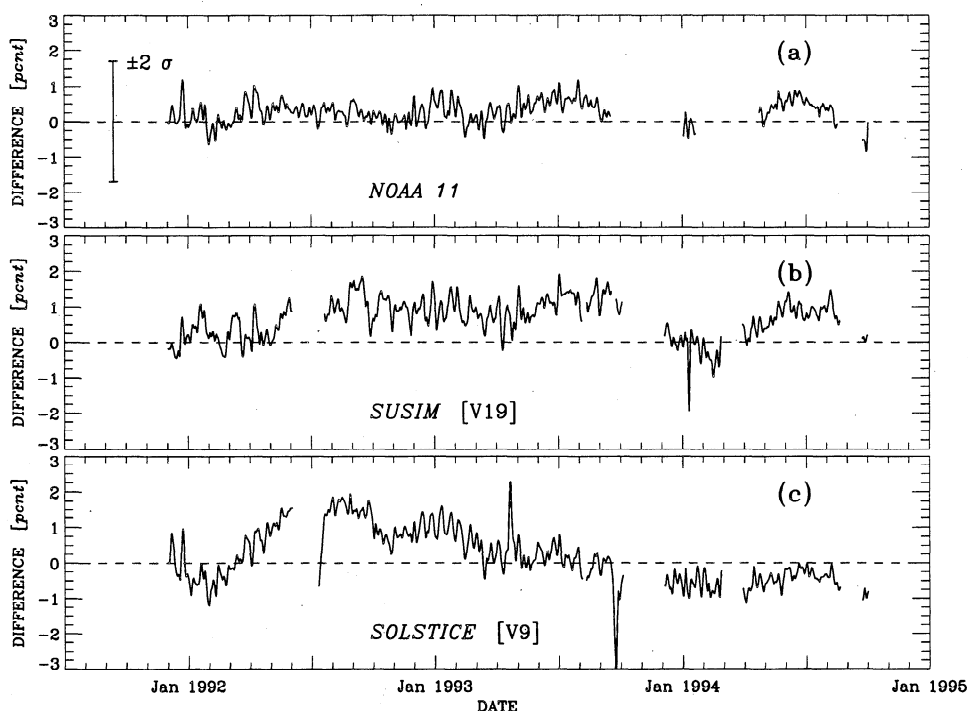


**Figure 10.** Desolarized time series at 200-208 nm: (a) NOAA 11, (b) SUSIM, and (c) SOLSTICE. All time series have been smoothed with a 5-day binomial average.

solar variations predicted by the NOAA 11 Mg II index and scale factors are not equivalent to the actual irradiance variations, is discussed further in section 6.

We can also evaluate the long-term behavior and spectral drift of each instrument for all wavelengths, using desolarized data and the plotting method of Plate 1. For each instrument, the data in each 10-nm band are normalized to the average of December 1-10, 1991. As noted in section 3, the impact of the Mg II proxy model is insignificant at most wavelengths longward of 290 nm ( $\Delta F_{\text{cycle}} < 0.5\%$ ), except for absorption lines such as Fe II and Ca II. The variations from these lines become negligible when 10-nm bands are used. The NOAA 11 desolarized results are shown in Plate 2.

Virtually all of the data show drifts of  $\pm 1\%$  or less (light green, yellow), with slightly larger changes in the 250-260 nm band (which is due to residual, uncorrected wavelength scale drift) and some data at  $\lambda < 200$  nm. As discussed in paper 1, the NOAA 11 irradiance data at 170-200 nm used a different long-term correction procedure for throughput change due to the lack of SSBUV irradiance data in this wavelength region, with increased uncertainty at the shortest wavelengths.

Plate 3 shows the SUSIM data, desolarized and plotted with the same method used for Plate 2. These data also have differences from the reference bin generally within the  $\pm 1\%$  range, increasing to  $+2\%$  (light blue) at 170-180 nm and  $-1.5-2\%$  at 260-270 nm. Rapid degradation in the SUSIM instrument response during the first 6 months of operation led to increased uncertainty in the instrument calibration during this period (L. E. Floyd, private communication, 1997). The SOLSTICE desolarized data presented in Plate 4 have drifts of  $\pm 1\%$  or less at 300-380 nm, but show larger drifts in other spectral regions. The data in the 260-300 nm region drift by  $-2\%$  or more, particularly at 280-300 nm (pink). Positive drifts are seen at 180-210 nm, reaching 2-3% at 180-190 nm (blue) before drifting downward later. Rottman and Woods [1994] showed that the SOLSTICE instrument has experienced 2-3 times more degradation in its F channel (180-300 nm) than in either the G (115-180 nm) or N (300-420 nm) channels. The largest drifts in Plate 4 correspond precisely to the boundaries of the F channel wavelength region, even when the wavelength band used for averaging is reduced to  $\Delta\lambda = 2$  nm. These changes appear to represent remaining uncorrected instrument drift in bands near the F channel boundaries.

We note that instruments measuring solar irradiance frequently experience larger drifts during the first year of operation. This behavior was observed for NOAA 11 (see Figure 11 of paper 1), but does not appear in Plate 2 because the time period was chosen to be coincident with the UARS observations.

The determination of the magnitude of long-term solar UV variation requires the definition of appropriate dates. Although the data sets used here do not reach solar minimum, they do cover most of the solar cycle range. Using February 1992 to September 1994 for our date limits and 27-day averaged data to remove the effects of rotational modulation, we conclude that the solar irradiance in the 200-208 nm band decreased by  $\sim 6-7\%$  during this period. Based on the results from all three instruments shown here, the accuracy of this number is approximately  $\pm 1.0-1.5\%$ , which is a factor of 2 improvement over previous measurements. It approaches the 1% long-term accuracy requirement needed to understand the role of solar forcing in middle atmosphere behavior. Our results are consistent with the results of Lean *et al.* [1992] derived from initial SUSIM measurements. Floyd *et al.* [1998] used extreme single dates in the UARS SUSIM data record through January 1996 to give solar irradiance variation estimates of 9-10% at 190-207 nm and 4-5% at 215-250 nm. They then used the NOAA 9 Mg II index of DeLand and Cebula [1998] to estimate a

solar cycle range of  $\Delta F \approx 12-14\%$  at 207 nm, which they stated to be significantly larger than the predictions of Lean *et al.* [1992]. However, Lean *et al.* [1992] and this paper both use a 27-day smoothed Mg II index for long-term predictions, which lowers the maximum range by  $\sim 3\%$  due to the removal of rotational modulation. We recommend the use of rotationally smoothed time series values when investigating the atmospheric impact of long-term solar variations. We note that DeLand and Cebula [1994] showed the maximum range of the daily NOAA 9 Mg II index during the rise of cycle 22 to be  $\sim 12\%$ , which when combined with the average scale factor presented earlier, gives a value for  $\Delta F_{\text{cycle}}(207 \text{ nm})$  consistent with that of Floyd *et al.* [1998].

## 6. Time Series Analysis

### 6.1. Periodograms

Further information about solar spectral irradiance variations can be obtained through statistical methods such as power spectral analysis. In this paper, we use the periodogram formulation derived by Scargle [1982] and modified by Horne and Baliunas [1986] to analyze the time series data. The periodogram technique is convenient for the solar irradiance data sets because it handles data gaps without filling or interpolation and successfully extracts periodic signals from noisy data. Examples of periodogram use in the literature include Baliunas *et al.* [1985], Lean and Brueckner [1989], Lean [1990], Cebula and DeLand [1998], and DeLand and Cebula [1998]. We note that unlike some other power spectral analysis techniques, the removal of a long-term trend before examining the time series data for short-term periodicities is not recommended because the resulting power values would then not be properly normalized [Horne and Baliunas, 1986].

Figure 11 shows the periodogram of the NOAA 11 SBUV/2 200-208 nm irradiance time series for the time interval February 1989 to October 1994, representing the complete NOAA 11 solar data record, using a set of 150 evenly spaced frequencies which correspond to periods between 10 and 50 days. The dashed line indicates a "false alarm probability" (FAP) of 0.1%, defined as the signal strength at which a peak has an 0.1% probability of being caused by statistical noise [Horne and Baliunas, 1986]. Using this criterion, we see that significant power is present at both 27 days and 29 days, corresponding to solar rotational modulation. There is also a small peak at  $\sim 13.5$  days which is below the FAP = 0.1% level. However, this does not mean that no 13-day periodicity occurred during 1989-1994, because the periodogram is evaluating power over the full time interval. Thus a high-frequency (short period) signal which lasts for a relatively small portion of the entire data interval may have a comparatively low power. Figure 12 presents NOAA 11 SBUV/2, UARS SUSIM, and UARS SOLSTICE periodograms at 200-208 nm for the dates of common measurements used for irradiance comparisons, December 1991 to September 1994. Reducing the periodogram time interval gives less power for NOAA 11 at 27 days (Figure 12a), because much less of the strong solar maximum rotational modulation is included. The peak at 29 days is now much weaker. The periodograms of the SUSIM and SOLSTICE 200-208 nm irradiance time series for the overlap period shown in Figures 12b and 12c, respectively, look very similar to the NOAA 11 periodogram, as expected. The UARS data seem to show slightly more power than NOAA 11 at 27 days and less at 29 days. We can evaluate the agreement between irradiance data and predicted solar variations by applying the periodogram technique to desolarized time series such as Figures 9 and 10. The periodogram results shown in Figure 13 for 200-208 nm have no peaks exceeding the 99.9% significance level for any

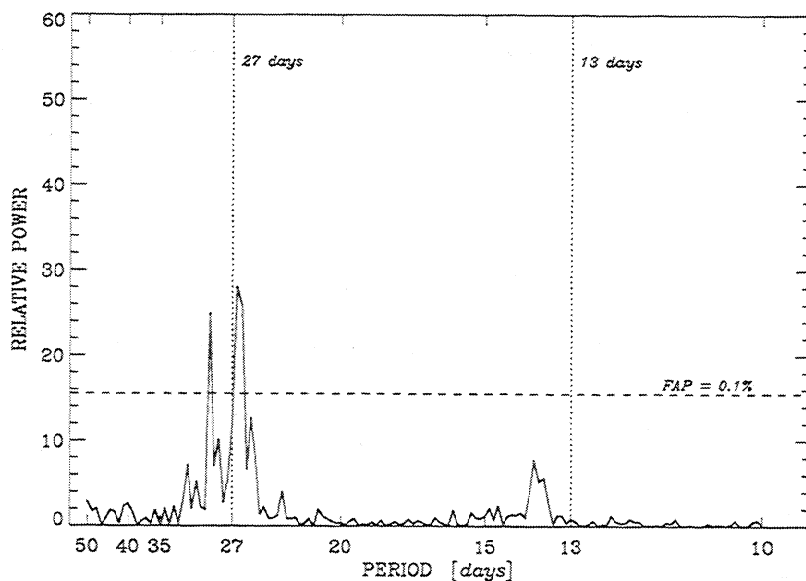


Figure 11. NOAA 11 periodogram of 200-208 nm irradiance data for December 1988 to October 1994, using periods of 10-50 days. The dashed line labeled "FAP = 0.1%" denotes 99.9% statistical significance, as discussed in the text.

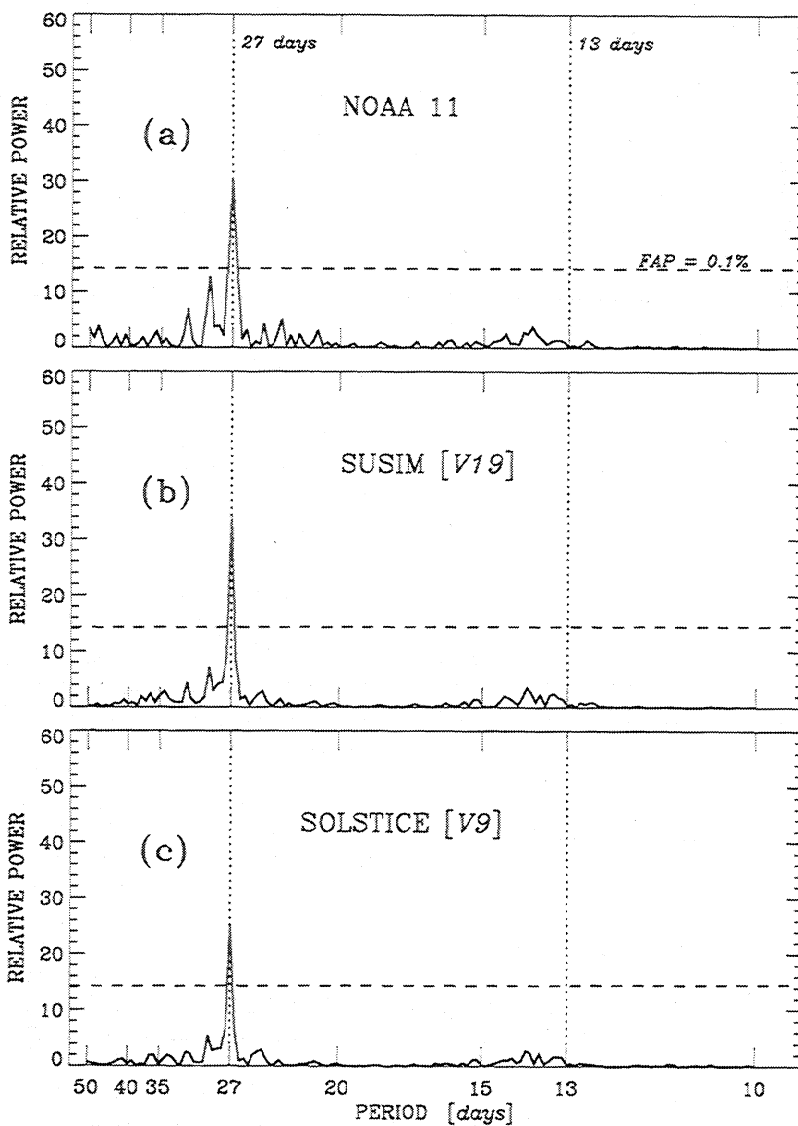


Figure 12. Periodograms of 200-208 nm data for December 1991 to September 1994, using periods of 10-50 days: (a) NOAA 11; (b) SUSIM; and (c) SOLSTICE.

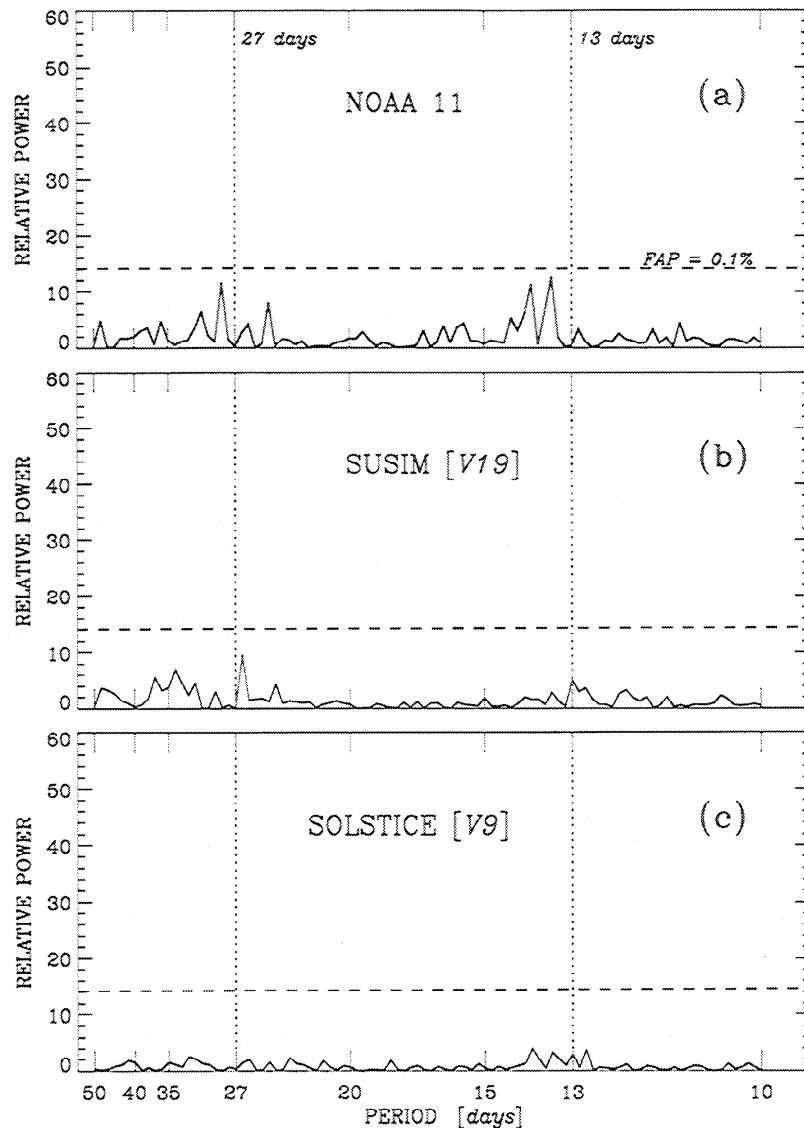


Figure 13. Periodograms of desolarized 200-208 nm data for December 1991 to September 1994, using periods of 10-50 days: (a) NOAA 11; (b) SUSIM; and (c) SOLSTICE.

instrument, but prominent features for NOAA 11 at ~14 days and 28 days. Periodograms of NOAA 11 desolarized data at other wavelengths show similar features in some cases, with reduced power levels from the 200-208 nm data. We plan further investigations into the spectral and temporal characteristics of this result.

## 6.2. Dynamic Power Spectra

Because the short-term periodicities in solar UV irradiance data evolve as active regions grow and die, we would like to examine changes in these periodicities with time. For this purpose, we have adapted the "dynamic power spectra" method utilized by Bower [1992]. We apply the periodogram to successive 256-day windows of data, stepping the window in increments of 64 days. These results can then be arranged as a function of period and time, allowing the evolution of specific periodicities to be tracked. Previous applications of the dynamic power spectra method to NOAA 11 SBUV/2, SOLSTICE, and SUSIM Mg II index data are shown by Cebula and DeLand [1998].

For NOAA 11 200-208 nm irradiance data, the dynamic power spectrum in Plate 5 shows that the double peak in the periodogram

of Figure 11 is created by a transition from 29-day to 26-day periodicity during 1989-1990, which then migrates to 27-day power during 1992 and 28-day power during 1993. During the course of each solar cycle, the average latitude at which active regions emerge decreases, leading to the possibility of changes in the nominal short-term period due to differential rotation. Observations of the He I 10830 Å equivalent width for cycle 21 by Harvey [1984] suggest that the evolution of large activity complexes is a much stronger effect. This is confirmed by Plate 5, in which the "rotational" period both increases and decreases during cycle 22. The slow drift of "preferred" active longitudes over several years could also lead to a shift in observed period [Foukal, 1990, p. 284]. The dynamic power spectrum illustrates the limitations of representing solar rotational variability at a constant period.

Using data which extended through the rise of cycle 22 in 1988, Pap et al. [1990] found that the 27-day power was consistently stronger in the declining phase of a solar cycle than in the rising phase for various solar indices. Plate 5 shows that in the NOAA 11 200-208 nm irradiance data, the strongest rotational modulation power occurs during the maximum of cycle 22. Maximum relative

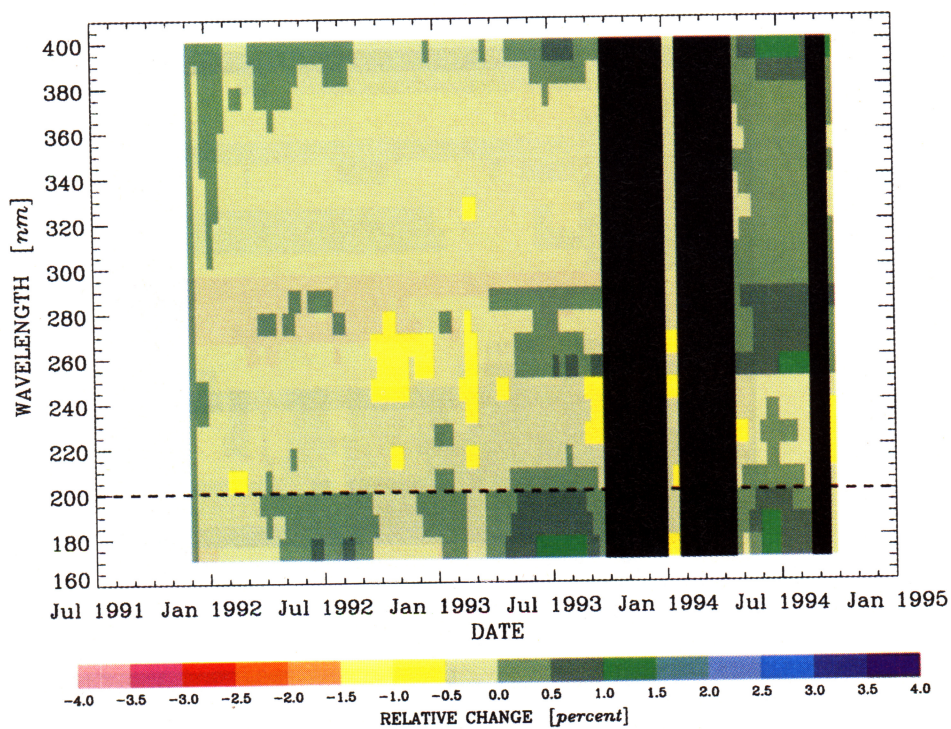


**Plate 2.** NOAA 11 spectral change using desolarized data from December 1991 to September 1994. Data are binned in 10-nm, 10-day increments, and normalized to the average of December 1-10, 1991. The dashed line has the same meaning as in Plate 1.

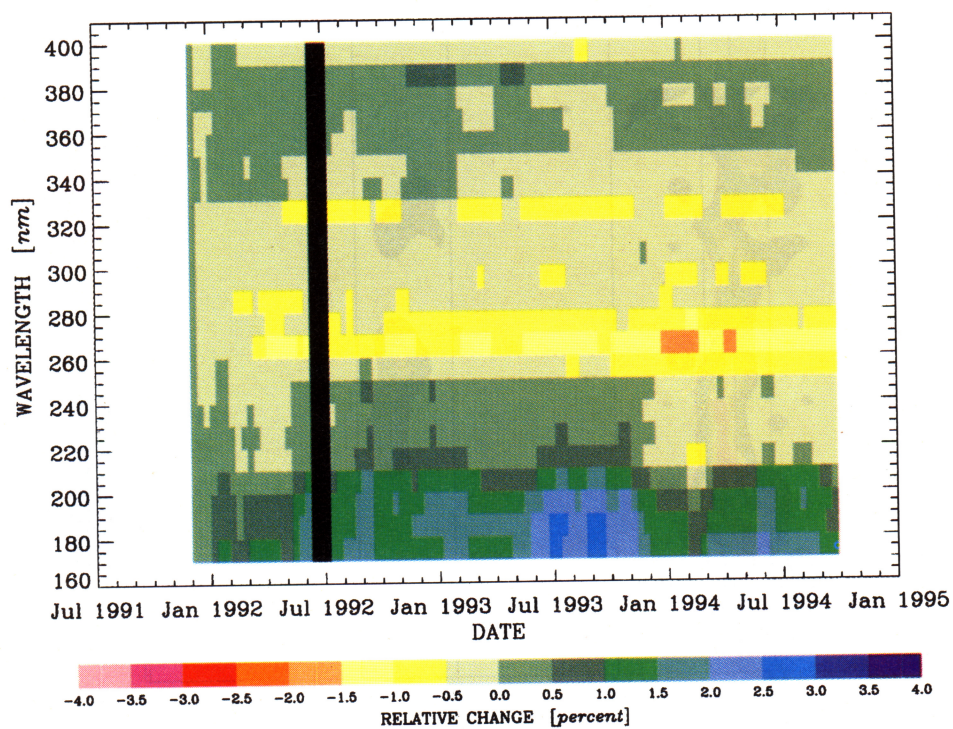


**Plate 3.** SUSIM spectral change using desolarized data from December 1991 to September 1994, normalized to December 1-10, 1991.

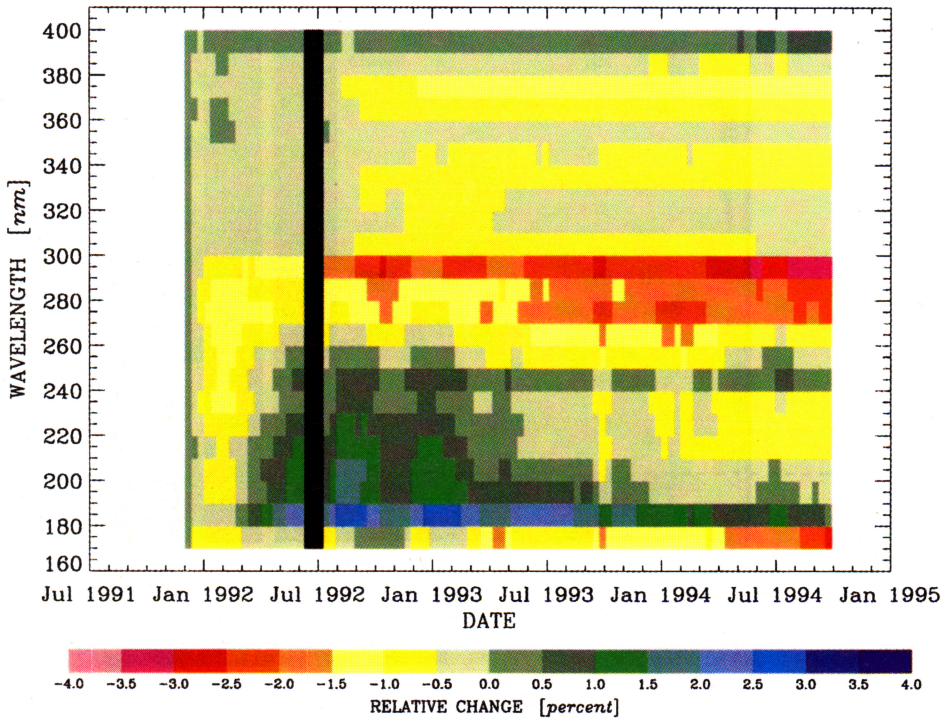


Plate 4. SOLSTICE spectral change using desolarized data from December 1991 to September 1994, normalized to December 1-10, 1991.

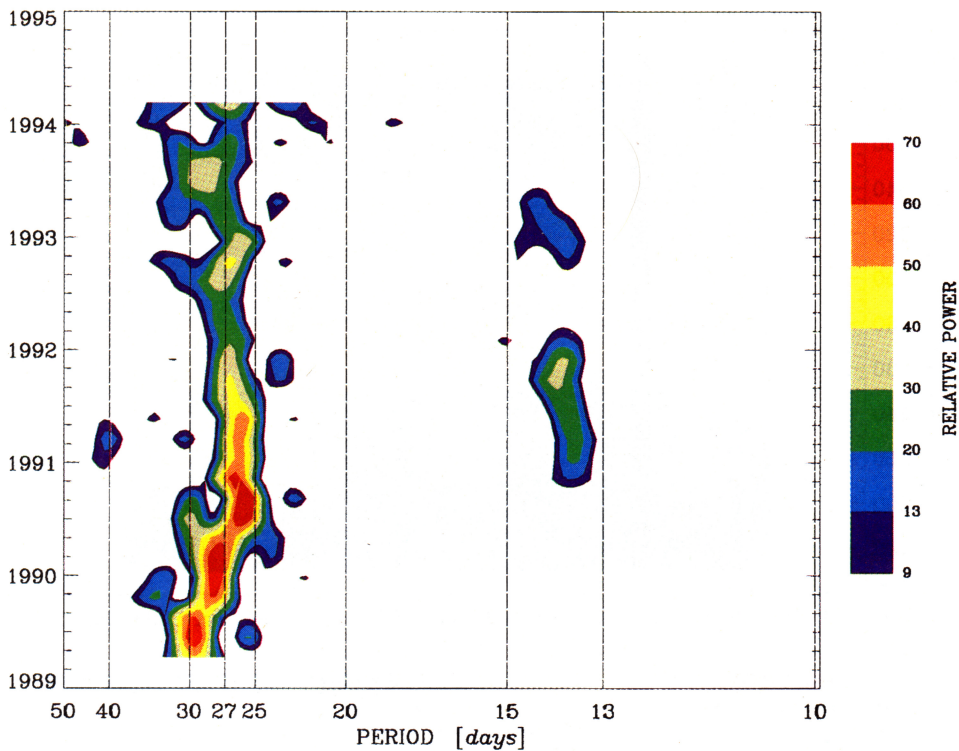


Plate 5. Dynamic power spectrum of NOAA 11 200-208 nm irradiance data for December 1988 to October 1994. Purple and blue contours correspond to FAP = 5% and 0.1%, respectively; additional color contours represent relative power levels consistent with Figure 11.

power values are greater than 60 during 1990, compared with maximum values of 30-40 during the declining phase in late 1992 and 1993. The dynamic power spectrum of the NOAA 11 Mg II index gives virtually identical results during the same measurement period [Cebula and DeLand, 1998]. However, the dynamic power spectrum of the NOAA 9 Mg II index data, which covers a full solar cycle, shows considerably more power in the declining phase of cycle 22 than in the rising phase, in agreement with Pap et al. [1990]. Continued study of this result will be valuable as solar activity moves into the increasing phase of cycle 23.

Plate 5 also shows a significant episode of 13-day periodicity during 1991, which is responsible for the small peak at this frequency in Figure 11. No other periods shorter than 26-29 days are found. Caligari et al. [1995] present a model of magnetic flux tube emergence which shows that the growth of a dominant mode with azimuthal wave number  $m = 2$  leads to surface active regions with  $\Delta\phi = 180^\circ$ . Comparison of the 200-208 nm results in Plate 5 with the dynamic power spectrum of the NOAA 11 discrete Mg II index presented by Cebula and DeLand [1998] shows strong similarities, although there is less power at 13-14 days in the Mg II index. This result is consistent with the conclusions of DeLand and Cebula [1998] based on analysis of short-term variations in NOAA 9 SBUV/2 data, as well as the work of Donnelly and Puga [1990] with Nimbus 7 SBUV data. The dynamic power spectra of the 200-208 nm time series from UARS SUSIM and SOLSTICE (not shown) are very similar in appearance to the NOAA 11 data in Plate 5, particularly in late 1992 where the main rotational period shifts to 25-26 days and some power appears at 14 days. This reinforces the visual impression of consistent behavior suggested by the time series of Figure 8.

6.3. Spectral Periodograms

Previous work by Donnelly [1988] with Nimbus 7 SBUV data during the maximum and declining phase of cycle 21 (1978-1984) showed that solar rotational modulation was temporally coherent over the 170-290 nm wavelength region during this time. We have performed a similar analysis for the NOAA 11 irradiance data during cycle 22, using the periodogram technique. Periodograms were calculated using 10-nm bands over the wavelength range 170-400 nm (centered at 175 nm, 185 nm, etc.), the UARS overlap interval (December 1991 to September 1994), and the same frequencies (i.e., periods) as Figure 11. No significant power was observed at any period outside the rotational modulation interval of 25-30 days. Therefore, for each wavelength band, we have summed the relative power values for all frequencies corresponding to this range of periods, then divided the result by 3 to reflect the approximate width in frequency space of the rotational modulation peak (see Figure 12). The results in Figure 14a show strong rotational periodicity in the NOAA 11 data, with roughly uniform power between 175 and 255 nm and diminishing strength out to 285 nm.

Figure 14b presents the same type of plot for the UARS SUSIM V19 irradiance data. These data show similar spectral characteristics to the NOAA 11 data, with slightly less power between 215 and 275 nm. Brueckner et al. [1996] suggest that irradiance data at wavelengths longward of ~300 nm can be anticorrelated with chromospheric activity and show examples of this for selected solar rotations in SUSIM data at 345-355 nm during late 1991 and early 1992. This idea is consistent with the blocking of heat flow to the photosphere by sunspots, thus causing a decrease in total solar irradiance [Foukal, 1990]. The amplitude of the features shown by Brueckner et al. [1996] appears to be ~0.3% peak-to-peak, which is comparable to the irradiance changes caused by large sunspot groups. We find no evidence for any persistent rotational modula-

tion signal in the SUSIM data longward of 300 nm from the periodogram analysis, in agreement with the NOAA 11 result. In Figure 14c, we see that the spectral periodogram of the SOLSTICE irradiance data is generally similar to the NOAA 11 and SUSIM results. However, the SOLSTICE results show less power at 215 and 285 nm than at 245 nm, in contrast to the results from NOAA 11 and SUSIM. We have no explanation for the difference in spectral structure at this time but hope to pursue this topic further.

6.4. Intermediate Periods

Solar rotational modulation (27-day, 13-day) and solar cycle (11-year) time scales are the most visible manifestations of solar UV activity. Other studies in the literature have focused on intermediate-length periods. Chandra [1989] found a 160-day period in 10.7-cm radio flux ( $F_{10.7}$ ) and Nimbus 7 SBUV 205-nm irradiance data during 1979-1984 and a 53-day period in  $F_{10.7}$ . Hoegy and Wolff [1989] identified 7-month and 5-month periods in solar EUV activity using Pioneer Venus photoemission current ( $I_{pe}$ ) data. Lean and Brueckner [1989] looked for 100-500 day periods during solar cycles 19-21 in  $F_{10.7}$ , sunspot blocking function ( $P_S$ ), sunspot number ( $R_Z$ ), and Ca II K plage index (PI), finding a clear signal at approximately 155 days in all data sets except PI and a weaker signal at 323 days. Lean [1990] extended the study of 155-day periods to cycles 12-21 using  $R_Z$  and sunspot group area. She found that the strength of this period appeared to follow an 11-year cycle, with the greatest power during maximum solar activity. Pap et al. [1990] examined multiple data sets (total irradiance ( $S$ ),  $F_{10.7}$ ,

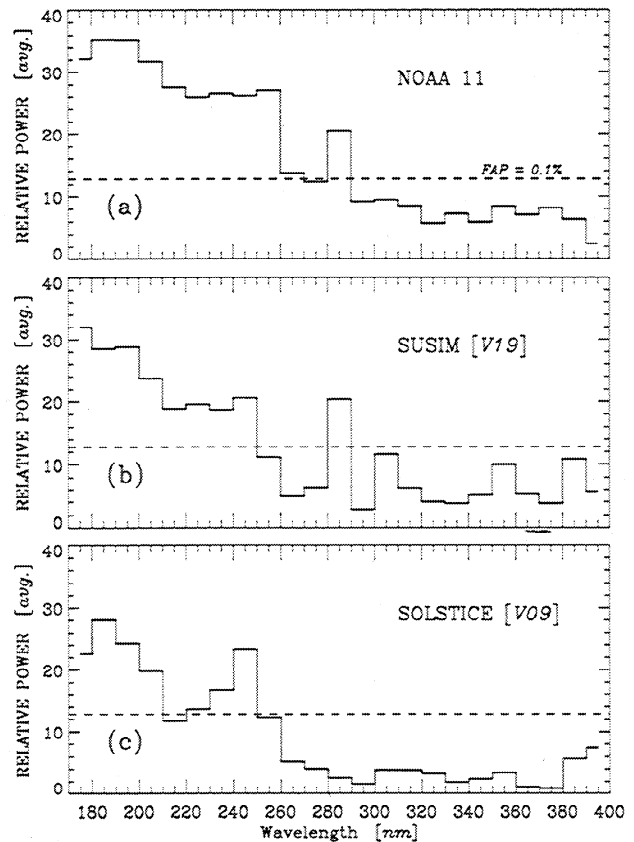
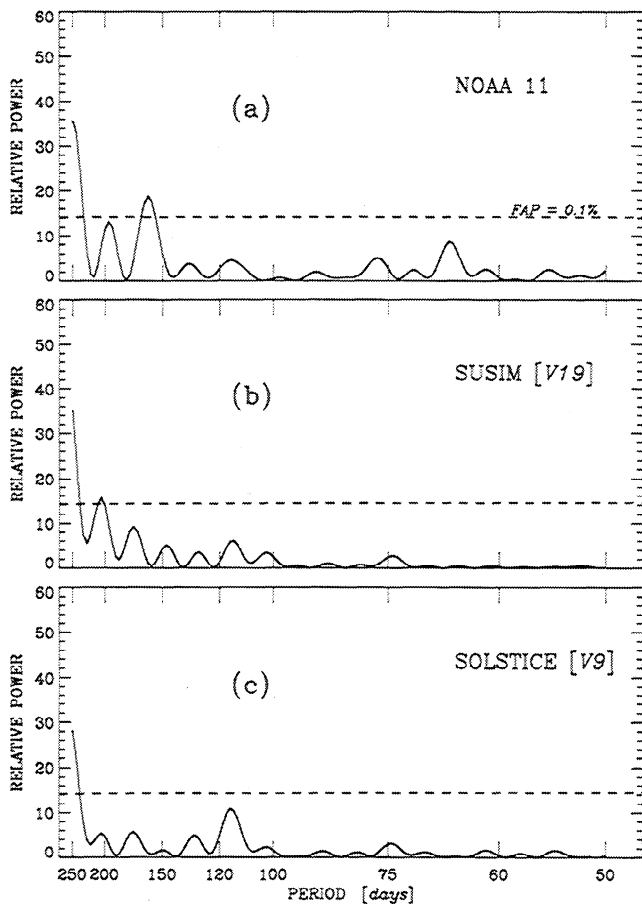


Figure 14. Spectral periodogram of irradiance data between 170 and 400 nm for December 1991 to September 1994: (a) NOAA 11; (b) SUSIM; and (c) SOLSTICE. The relative power in each panel represents the average of all periods between 25 and 30 days, as discussed in the text.

Ca K plage, SME Ly  $\alpha$ , Nimbus 7 Mg II) for cycle 21 and longer where available. Periods of 51 days and 150-157 days were determined for total irradiance and some sunspot indices, and longer periods in the 240-330 day range were also claimed. Bower [1992, p. 385] found occasional evidence for both 51-52 day and 154 day periods in a similar study, but noted that such signatures "...could be the result of a coincidental occurrence of one or more non-periodic waveforms..." rather than representing persistent periodic behavior. Watari [1995] used fractal analysis of data from solar cycles 20 and 21 to show that solar activity variations were irregular for timescales between several days and several months. Recently, Zhou *et al.* [1997] identified a 60-80 day periodicity in the SOLSTICE V08 irradiance data (175-210 nm, 200-205 nm, Mg II index), as well as in the UARS MLS ozone data between 3 and 10 mbar.

We searched for intermediate solar periodicities in the NOAA 11, SUSIM, and SOLSTICE irradiance data at periods between 50 and 250 days, using 150 frequencies in the periodogram analysis and the interval December 1991 to September 1994. Figure 15 shows that for the 200-208 nm band, statistically significant power was found at ~160 days for NOAA 11 but not in the SUSIM V19 or SOLSTICE V09 data. The significance of the NOAA 11 160-day peak falls below 99.9% for different choices of starting date between 1989 and 1991. We also found no intermediate-term periodicities at 200-208 nm using SOLSTICE V08 data. This result is inconsistent with the analysis of Zhou *et al.* [1997]. However, Figure 16 shows that periodograms of irradiance time series at 350-



**Figure 15.** Periodograms of 200-208 nm data for December 1991 to September 1994, using periods of 50-250 days: (a) NOAA 11; (b) SUSIM; and (c) SOLSTICE.

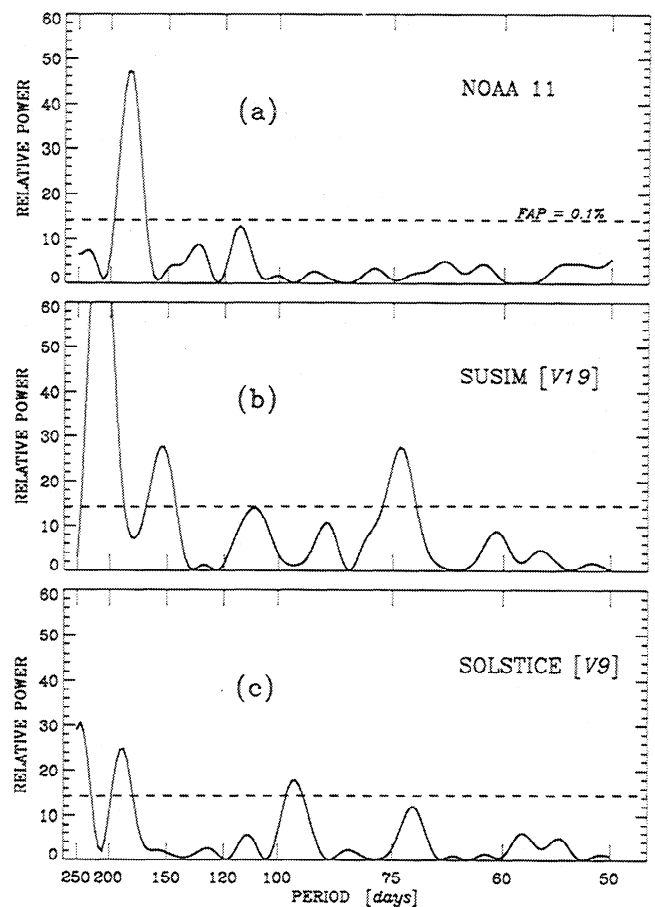


**Figure 16.** Periodograms of 350-360 nm data for December 1991 to September 1994, using periods of 50-250 days: (a) NOAA 11; (b) SUSIM; and (c) SOLSTICE.

360 nm produced significant periodicities at ~180 days for NOAA 11, ~210, 160, and 75 days for SUSIM, and 180 and ~95 days for SOLSTICE. These peaks are somewhat unexpected, since solar variability is predicted to be very small at wavelengths greater than 300 nm. It is difficult to try to confirm the validity of such periods using the dynamic power spectrum method because the periods of interest represent a significant fraction of the overall data set length (1037 days for the NOAA 11 and UARS overlap period used here). Increasing the periodogram window size to 384 days to accommodate longer test periods still allows only 3-5 cycles of the periods mentioned here, so that spurious events in the irradiance data can generate a disproportionately large response.

The spectral periodogram method provides additional information about the intermediate-term periodicities shown in Figures 15 and 16. Results for all wavelength bands and periods are shown for NOAA 11 data in Figure 17, where the minimum surface level corresponds to the 99.9% significance level in previous plots. The NOAA 11 data display significant power at ~180 days for all wavelength bands longward of 265 nm, maximizing at ~330 nm.

This result likely reflects a residual error of ~0.5% in the NOAA 11 goniometric correction, corresponding to the seasonal cycle of the spacecraft-centered azimuth angle. Some power is also evident at 170-240 nm with a period of ~160 days, as noted earlier. Results for the SUSIM data in Figure 18 show power at 70-75 and ~110 days for wavelength bands between 330 and 390 nm, with considerable power at ~150 days and 200-250 days. Some of this power may be related to the timing of the SUSIM reference calibrations, which have generally occurred at intervals of ~200( $\pm$ 20) days

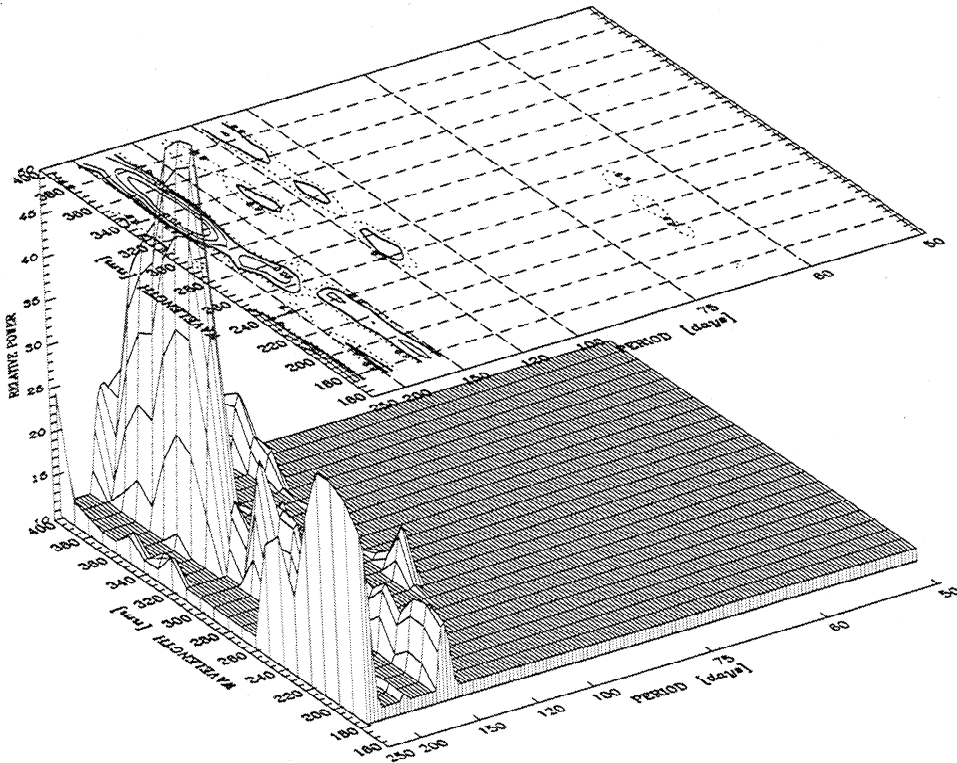


Figure 17. Spectral periodogram of NOAA 11 irradiance data for December 1991 to September 1994, using long periods (50-250 days). The minimum surface level represents 99.9% statistical significance.

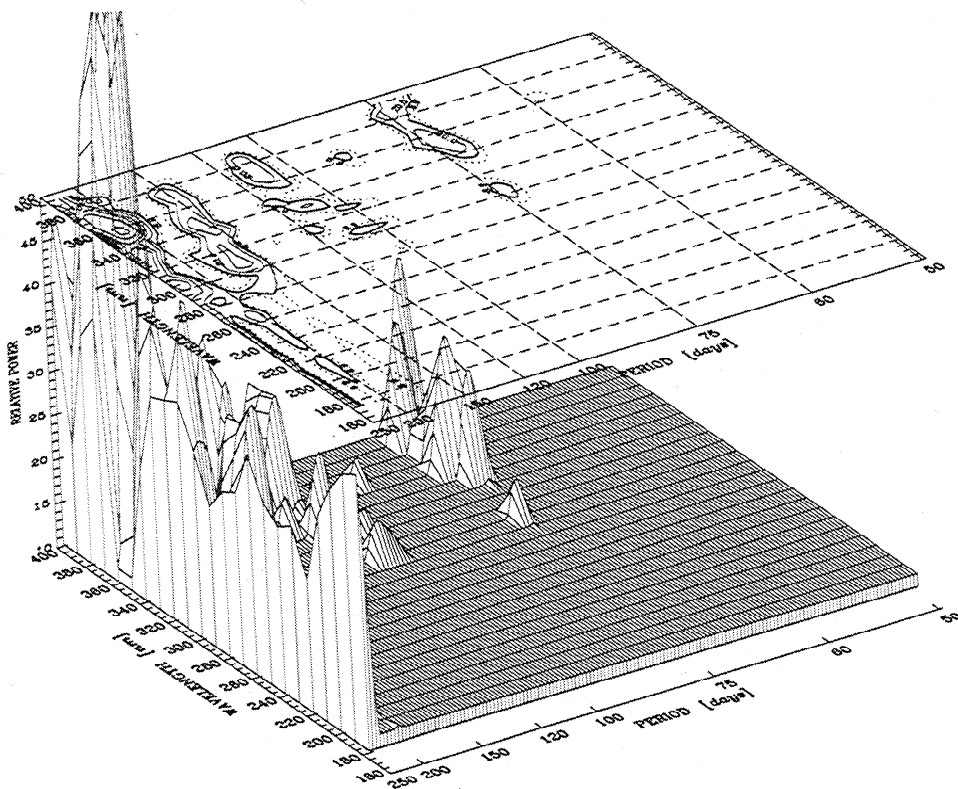


Figure 18. Spectral periodogram of SUSIM irradiance data for December 1991 to September 1994, using long periods (50-250 days).

between March 1992 and January 1996 [Floyd *et al.*, 1996]. Results for the SOLSTICE data in Figure 19 show power at  $\sim 115$  days between 260-300 nm, and periods of approximately 220-250 days for 170-240 and 300-400 nm. In all cases, the power is relatively small. For all three instruments, the results are very sensitive to the choice of data interval, as discussed earlier in section 6.4. We note that a similar analysis of the SOLSTICE V08 data showed substantial power at  $\sim 72$  days between 210-290 nm and 300-350 nm, with very strong peaks at 310-320 and 370-380 nm. UARS reverses orientation approximately every 36 days ("yaw maneuver") to keep the proper pointing for the spacecraft solar panels, so such a period could represent a signature of that effect in irradiance data. The changes in pointing accuracy caused by each UARS yaw maneuver have spectrally dependent effects on the wavelength calibration and field of view sensitivity of SUSIM and SOLSTICE [Woods *et al.*, 1996]. The lack of physical justification for persistent solar UV activity periods in the range 50-250 days makes it difficult to ascribe their presence in periodogram analyses to true solar variations.

The differences in period length and spectral location for the periodogram results shown in Figures 17-19 strongly suggest that true intermediate term periodicities are difficult to identify in solar spectral irradiance data. Inspection of time series plots such as Figure 6 indicates that any periodic behavior at long wavelengths has an amplitude of 0.5% or less, which approaches or exceeds the accuracy of instrument throughput corrections. No instrument showed any persistent spectral power for 50-250 day periods at  $\lambda < 260$  nm, where upper photospheric and chromospheric solar activity should be evident. A separate analysis of the Mg II index time series from NOAA 9, NOAA 11, SUSIM, and SOLSTICE showed no significant power in any of these data sets for periods greater than 27 days. Because it is an irradiance ratio, the Mg II index is less likely to be impacted by the processing artifacts that can

influence irradiance data. Since no two instruments duplicated a significant period and spectral location for intermediate-term periodicities, we are inclined to attribute the results shown in Figures 17-19 to aspects of the long-term instrument characterization and/or data analysis for each instrument. In particular, the 60-80 day period in SOLSTICE V08 irradiance data identified by Zhou *et al.* [1997] appears to be an artifact. Although they did filter their data sets with a 36-day band pass to remove apparent yaw-related signals in the MLS ozone data, our results suggest that there may be other such signatures in these data. These results emphasize the difficulties associated with searching for subtle irradiance variations and the value of having multiple independent data sets for the identification and analysis of periodic behavior, as well as the evaluation of long-term changes in the solar spectral irradiance.

## 7. Conclusions

Solar spectral UV irradiance data from the NOAA 11 SBUV/2 instrument are now available for the period December 1988 to October 1994. Long-term smoothed irradiance changes during this interval, which includes the maximum and declining phase of solar cycle 22, are  $<1\%$  longward of 300 nm,  $-(3-4)\%$  at 240-250 nm, and  $-(6-7)\%$  at 200-208 nm. The NOAA 11 SBUV/2 results are very consistent with irradiance data from UARS SUSIM and SOLSTICE throughout their 3-year overlap, with long-term accuracies of approximately  $\pm 1.0-1.5\%$ . Some fluctuations do appear in the SUSIM and SOLSTICE data during the first year of UARS operation (December 1991 to July 1992), while the NOAA 11 data are impacted by orbit drift effects during its last year of solar measurements (September 1993 to October 1994). All three instruments show similar short-term periodic behavior corresponding to rotational modulation. Dynamic power spectra of the NOAA 11 data verify the evolutionary nature of solar rotational activity at

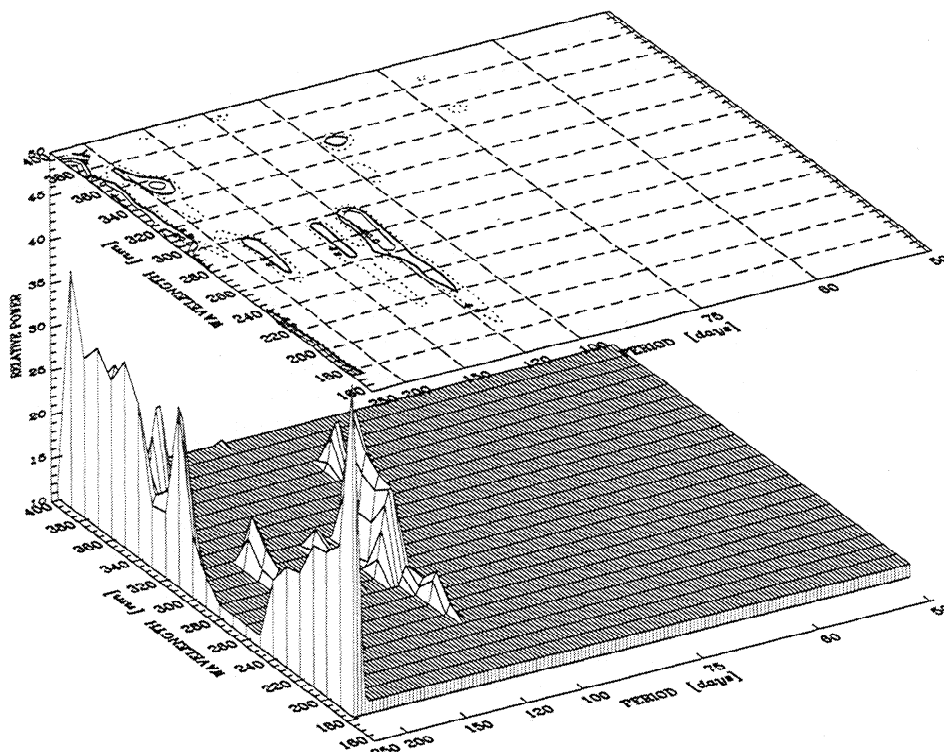


Figure 19. Spectral periodogram of SOLSTICE irradiance data for December 1991 to September 1994, using long periods (50-250 days).

different phases of the solar cycle with respect to both strength and amplitude. Periodogram analysis for longer periods (50-250 days) shows substantial spectral and temporal differences between all three data sets. We do not see any conclusive evidence for true solar activity at any periods in this range within the precision of the data sets.

The NOAA 11 spectral irradiance data provide an additional 2.5 years of data during the maximum of Cycle 22 to complement the UARS instruments' data sets. (The NOAA 11 irradiance data and supporting documentation are available on-line via anonymous FTP at [ssbuv.gsfc.nasa.gov/pub/solar/sbuv2/noaa11](http://ssbuv.gsfc.nasa.gov/pub/solar/sbuv2/noaa11) or through the SBUV/2-SSBUV WWW site at <http://ssbuv.gsfc.nasa.gov/solar.html>). We plan to develop similar instrument change corrections for NOAA 9 SBUV/2, so that spectral irradiance data will be available for all of solar cycle 22. Three additional SBUV/2 instruments are scheduled for launch between approximately 1999-2003, which should provide solar UV data for cycle 23 as well.

**Acknowledgments.** Walt Planet and Dudley Bowman of NOAA NESDIS provided the raw NOAA 11 SBUV/2 data. Irradiance data for the comparisons presented here were supplied by Linton Floyd and Dianne Prinz (UARS SUSIM), Gary Rottman and Tom Woods (UARS SOLSTICE), Michael VanHoosier (ATLAS SUSIM), and Gerard Thullier (ATLAS SOLSPEC). We gratefully acknowledge the contributions of two anonymous reviewers, in particular for their clarification and guidance on solar physics and UARS operations issues. We thank Ernest Hilsenrath for constructive comments on the paper. We also thank Linton Floyd for valuable discussions regarding the UARS SUSIM data. L. P. DeLand provided graphic assistance. This research was supported by NASA grant NASW-4864.

## References

- Ackerman, M., Solar ultraviolet flux below 50 kilometers, *Can. J. Chem.*, **52**, 1505-1509, 1974.
- Ahmad, Z., M. T. DeLand, R. P. Cebula, H. Weiss, C. G. Wellemeier, W. G. Planet, J. H. Lienesch, H. D. Bowman, A. J. Miller, and R. M. Nagatani, Accuracy of total ozone retrieval from NOAA SBUV/2 measurements: Impact of instrument performance, *J. Geophys. Res.*, **99**, 22,975-22,984, 1994.
- Baliunas, S. L., et al., Time-series measurements of chromospheric Ca II H and K emission in cool stars and the search for differential rotation, *Astrophys. J.*, **294**, 310-325, 1985.
- Baum, W. A., F. S. Johnson, J. J. Oberly, C. C. Rockwood, C. V. Strain, and R. Tousey, Solar ultraviolet spectrum to 88 kilometers, *Phys. Rev.*, **70**, 781-782, 1946.
- Bojkov, R. D., L. Bishop, and V. E. Fioletov, Total ozone trends from quality-controlled ground-based data (1964-1994), *J. Geophys. Res.*, **100**, 25,867-25,876, 1995.
- Bouwer, S. D., Periodicities of solar irradiance and solar activity indices, II, *Sol. Phys.*, **142**, 365-389, 1992.
- Brasseur, G., The response of the middle atmosphere to long-term and short-term solar variability: A two-dimensional model, *J. Geophys. Res.*, **98**, 23,079-23,091, 1993.
- Broadfoot, A. L., The solar spectrum 2100-3200 Å, *Astrophys. J.*, **173**, 681-689, 1972.
- Brueckner, G. E., K. L. Edlow, L. E. Floyd, J. Lean, and M. E. VanHoosier, The Solar Ultraviolet Spectral Irradiance Monitor (SUSIM) experiment on board the Upper Atmosphere Research Satellite (UARS), *J. Geophys. Res.*, **98**, 10,695-10,711, 1993.
- Brueckner, G. E., L. E. Floyd, P. A. Lund, D. K. Prinz, and M. E. VanHoosier, Solar ultraviolet spectral-irradiance observations from the SUSIM-UARS experiment, *Metrologia*, **32**, 661-665, 1996.
- Caligari, P., F. Moreno-Inseris, and M. Schüssler, Emerging flux tubes in the solar convection zone, I, Asymmetry, tilt, and emergence latitude, *Astrophys. J.*, **441**, 886-902, 1995.
- Callis, L. B., M. Natarajan, J. D. Lambeth, and R. E. Bougher, On the origin of midlatitude ozone changes: Data analysis and simulations for 1979-1993, *J. Geophys. Res.*, **102**, 1215-1228, 1997.
- Cebula, R. P., and M. T. DeLand, Comparisons of the NOAA 11 SBUV/2, UARS SOLSTICE, and UARS SUSIM Mg II solar activity proxy indexes, *Sol. Phys.*, **177**, 117-132, 1998.
- Cebula, R. P., and E. Hilsenrath, Ultraviolet solar irradiance measurements from the SSBUV-1 and SSBUV-2 missions, in *Proceedings of the Workshop on the Solar Electromagnetic Radiation Study for Solar Cycle 22*, edited by R. F. Donnelly, pp. 250-264, NOAA Environ. Res. Lab., Space Environ. Lab., Boulder, Colo., 1992.
- Cebula, R. P., H. Park, and D. F. Heath, Characterization of the Nimbus 7 SBUV radiometer for the long-term monitoring of stratospheric ozone, *J. Atmos. Ocean. Technol.*, **5**, 215-227, 1988.
- Cebula, R. P., M. T. DeLand, and B. M. Schlessinger, Estimates of solar ultraviolet variability using the solar backscatter ultraviolet (SBUV) 2 Mg II index from the NOAA 9 satellite, *J. Geophys. Res.*, **97**, 11,613-11,620, 1992.
- Cebula, R. P., E. Hilsenrath, and M. T. DeLand, Middle ultraviolet solar spectral irradiance measurements, 1985-1992, from the SBUV/2 and SSBUV instruments, in *The Sun as a Variable Star*, edited by J. M. Pap et al., pp. 81-88, Cambridge Univ. Press, New York, 1994.
- Cebula, R. P., G. O. Thullier, M. E. VanHoosier, E. Hilsenrath, M. Herse, G. E. Brueckner, and P. C. Simon, Observations of the solar irradiance in the 200-350 nm interval during the ATLAS-1 mission: A comparison among three sets of measurements-SSBUV, SOLSPEC, and SUSIM, *Geophys. Res. Lett.*, **23**, 2289-2292, 1996.
- Cebula, R. P., L. K. Huang, and E. Hilsenrath, SSBUV sensitivity drift determined using solar spectral irradiance measurements, *Metrologia*, in press, 1998.
- Cebula, R. P., M. T. DeLand, and E. Hilsenrath, NOAA 11 Solar Backscatter Ultraviolet, model 2 (SBUV/2) instrument solar spectral irradiance measurements in 1989-1994, 1. Observations and long-term calibration, *J. Geophys. Res.*, this issue.
- Chandra, S., A search for five month solar induced periodicity in the stratosphere, *Geophys. Res. Lett.*, **16**, 711-714, 1989.
- Chandra, S., and R. D. McPeters, The solar cycle variation of ozone in the stratosphere inferred from the Nimbus 7 and NOAA 11 satellites, *J. Geophys. Res.*, **99**, 20,665-20,771, 1994.
- Chandra, S., J. L. Lean, O. R. White, D. K. Prinz, G. J. Rottman, and G. E. Brueckner, Solar UV irradiance variability during the declining phase of the solar cycle 22, *Geophys. Res. Lett.*, **22**, 2481-2484, 1995.
- DeLand, M. T., and R. P. Cebula, Composite Mg II solar activity index for solar cycles 21 and 22, *J. Geophys. Res.*, **98**, 12,809-12,823, 1993.
- DeLand, M. T., and R. P. Cebula, Comparisons of the Mg II index products from the NOAA 9 and NOAA 11 SBUV/2 instruments, *Sol. Phys.*, **152**, 61-68, 1994.
- DeLand, M. T., and R. P. Cebula, Solar UV activity at solar cycle 21 and 22 minimum from NOAA 9 SBUV/2 data, *Sol. Phys.*, **177**, 105-116, 1998.
- Donnelly, R. F., Uniformity in solar UV flux variations important to the stratosphere, *Ann. Geophys.*, **6**(4), 417-424, 1988.
- Donnelly, R. F., and L. C. Puga, Thirteen-day periodicity and the center-to-limb dependence of UV, EUV, and X-ray emission of solar activity, *Sol. Phys.*, **130**, 369-390, 1990.
- Donnelly, R. F., O. R. White, and W. C. Livingston, The solar Ca II K index and the Mg II core-to-wing ratio, *Sol. Phys.*, **152**, 69-76, 1994.
- Fleming, E. L., S. Chandra, C. H. Jackman, D. B. Considine, and A. R. Douglass, The middle atmospheric response to short and long term solar UV variations: Analysis of observations and 2-D model results, *J. Atmos. Terr. Phys.*, **57**, 333-365, 1995.
- Flieg, A. J., K. F. Klenk, P. K. Bhartia, K. D. Lee, C. G. Wellemeier, and V. G. Kaveeshwar, Vertical ozone profile results from the Nimbus 4 UV data, in *Proceedings, Fourth Conference on Atmospheric Radiation*, pp. 20-26, Amer. Meteor. Soc., Boston, 1981.
- Floyd, L. E., L. C. Herring, D. K. Prinz, and G. E. Brueckner, Maintaining calibration during the long term space flight of the Solar Ultraviolet Spectral Irradiance Monitor (SUSIM), *Proc. SPIE Int. Soc. Opt. Eng.*, **2831**, 36-47, 1996.
- Floyd, L. E., P. A. Reiser, P. C. Crane, L. C. Herring, D. K. Prinz, and G. E. Brueckner, Solar cycle 22 UV spectral irradiance variability: Current measurements by SUSIM UARS, *Sol. Phys.*, **177**, 79-87, 1998.
- Foukal, P., *Solar Astrophysics*, 475 pp., John Wiley, New York, 1990.
- Fowler, W. F., Spectral sensitivity characteristic of the SBUV/2 instrument—Differences in air and vacuum, *Rep. Ball SER SBUV-WF-94-749*, Ball Aerospace, Boulder, Colo., Sept. 6, 1994.

- Frederick, J. E., R. P. Cebula, and D. F. Heath, Instrument characterization for the detection of long-term changes in stratospheric ozone: An analysis of the SBUV/2 radiometer, *J. Atmos. Ocean Technol.*, **3**, 472-480, 1986.
- Hall, L. A., Solar variability in the spectral range 2350-2870 Å, *J. Geophys. Res.*, **88**, 6797-6799, 1983.
- Hall, L. A., and G. P. Anderson, Solar ultraviolet variation between 1977 and 1983, *J. Geophys. Res.*, **89**, 7322, 1984.
- Harvey, J. W., Helium 10830 Å irradiance: 1975-1983 in *Solar Irradiance Variations on Active Region Time Scales*, edited by B. J. Labonte et al., *NASA Conf. Publ.*, CP-2310, 197-211, 1984.
- Harvey, J. W., and W. C. Livingston, Variability of the solar He I 10830 Å triplet, in *Infrared Solar Physics*, edited by D. M. Rabin, J. T. Jefferies, and C. Lindsey, pp. 59-64, Kluwer Acad., Norwell, Mass., 1994.
- Heath, D. F., Observations of the intensity and variability of the near ultraviolet solar flux from the Nimbus 3 satellite, *J. Atmo. Sci.*, **26**, 1157-1160, 1969.
- Heath, D. F., Space observations of the variability of solar irradiance in the near and far ultraviolet, *J. Geophys. Res.*, **78**, 2779-2792, 1973.
- Heath, D. F., and B. M. Schlesinger, The Mg 280-nm doublet as a monitor of changes in solar ultraviolet irradiance, *J. Geophys. Res.*, **91**, 8672-8682, 1986.
- Heath, D. F., and M. P. Thekaekara, The solar spectrum between 1200 and 3000 Å, in *The Solar Output and Its Variation*, edited by O. R. White, pp. 193-212, Colo. Assoc. of Univ. Press, Boulder, 1977.
- Heath, D. F., A. J. Krueger, H. A. Roeder, and B. D. Henderson, The Solar Backscatter Ultraviolet and Total Ozone Mapping Spectrometer (SBUV/TOMS) for Nimbus G, *Opt. Eng.*, **14**, 323-331, 1975.
- Herman, J. R., R. D. Hudson, and G. Serafino, Analysis of the 8-year trend in ozone depletion from empirical models of solar backscattered ultraviolet instrument degradation, *J. Geophys. Res.*, **95**, 7403-7416, 1990.
- Heroux, L., and R. A. Swirbalus, Full-disk solar fluxes between 1230 and 1940 Å, *J. Geophys. Res.*, **81**, 436-440, 1976.
- Hilsenrath, E., D. Williams, and J. Frederick, Calibration of long term data sets from operational satellites using the space shuttle, *Proc. SPIE Int. Soc. Opt. Eng.*, **924**, 215-222, 1988.
- Hilsenrath, E., R. P. Cebula, M. T. DeLand, K. Laamann, S. Taylor, C. Wellemeyer, and P. K. Bhartia, Calibration of the NOAA 11 SBUV/2 ozone data set from 1989 to 1993 using in-flight calibration data and SSBUV, *J. Geophys. Res.*, **100**, 1351-1366, 1995.
- Hinteregger, H. E., EUV fluxes in the solar spectrum below 2000 Å, *J. Atmos. Terr. Phys.*, **38**, 791-806, 1976.
- Hoegy, W. R., and C. L. Wolff, A seven-month solar cycle observed with the Langmuir probe on Pioneer Venus Orbiter, *J. Geophys. Res.*, **94**, 8663-8671, 1989.
- Hood, L. L., The solar cycle variation of total ozone: Dynamical forcing in the lower stratosphere, *J. Geophys. Res.*, **102**, 1355-1370, 1997.
- Horne, J. H., and S. L. Baliunas, A prescription for period analysis of unevenly sampled time series, *Astrophys. J.*, **302**, 757-763, 1986.
- Hoyt, D. V., The Smithsonian Astrophysical Observatory solar constant program, *Rev. Geophys.*, **17**, 427-458, 1979.
- Jackman, C. H., E. L. Fleming, S. Chandra, D. B. Considine, and J. E. Rosenfield, Past, present, and future modeled ozone trends with comparisons to observed trends, *J. Geophys. Res.*, **101**, 28,753-28,767, 1996.
- Kariyappa, R., and K. R. Sivaraman, Variability of the solar chromospheric network over the solar cycle, *Sol. Phys.*, **152**, 139-144, 1994.
- Keating, G. M., G. P. Brasseur, L. S. Chiou, and N. C. Hsu, Estimating 11-year solar UV variations using 27-day response as a guide to isolate trends in total column ozone, *Adv. Space Res.*, **14**(9), 199-209, 1994.
- Labs, D., H. Neckel, P. C. Simon, and G. Thuillier, Ultraviolet solar irradiance measurement from 200 to 358 nm during Spacelab 1 mission, *Sol. Phys.*, **107**, 203-219, 1987.
- Lean, J., Solar ultraviolet irradiance variations: A review, *J. Geophys. Res.*, **92**, 839-868, 1987.
- Lean, J., Evolution of the 155 day periodicity in sunspot areas during solar cycles 12 to 21, *Astrophys. J.*, **363**, 718-727, 1990.
- Lean, J., Variations in the Sun's radiative output, *Rev. Geophys.*, **29**, 505-535, 1991.
- Lean, J. L., and G. E. Brueckner, Intermediate-term solar periodicities: 100-500 days, *Astrophys. J.*, **337**, 568-578, 1989.
- Lean, J., M. VanHoosier, G. Brueckner, D. Prinz, L. Floyd, and K. Edlow, SUSIM/UARS observations of the 120 to 300 nm flux variations during the maximum of the solar cycle: Inferences for the 11-year cycle, *Geophys. Res. Lett.*, **19**, 2203-2206, 1992.
- Lean, J. L., G. J. Rottman, H. L. Kyle, T. N. Woods, J. R. Hickey, and L. C. Puga, Detection and parameterization of variations in solar mid- and near-ultraviolet radiation (200-400 nm), *J. Geophys. Res.*, **102**, 29,939-29,956, 1997.
- McCormack, J. P., and L. L. Hood, Apparent solar cycle variations of upper stratospheric ozone and temperature: Latitude and seasonal dependences, *J. Geophys. Res.*, **101**, 20,933-20,944, 1996.
- Mentall, J. E., and D. E. Williams, Solar ultraviolet irradiances on December 7, 1983, and December 10, 1984, *J. Geophys. Res.*, **93**, 735-746, 1988.
- Mentall, J. E., J. E. Frederick, and J. R. Herman, The solar spectral irradiance from 200 to 300 nm, *J. Geophys. Res.*, **86**, 9881-9884, 1981.
- Mentall, J. E., B. Guenther, and D. Williams, The solar spectral irradiance between 150 and 200 nm, *J. Geophys. Res.*, **90**, 2265-2271, 1985.
- Mount, G. H., and G. J. Rottman, The solar absolute spectral irradiance 1200-3184 Å near solar maximum: July 15, 1980, *J. Geophys. Res.*, **86**, 9193-9198, 1981.
- Mount, G. H., and G. J. Rottman, The solar absolute spectral irradiance 1150-3175 Å: May 17, 1982, *J. Geophys. Res.*, **88**, 5403-5410, 1983a.
- Mount, G. H., and G. J. Rottman, The solar absolute spectral irradiance at 1216 Å and 1800-3173 Å: January 12, 1983, *J. Geophys. Res.*, **88**, 6807-6811, 1983b.
- Pap, J., W. K. Tobiska, and S. D. Bouwer, Periodicities of solar irradiance and solar activity indices, I, *Sol. Phys.*, **129**, 165-189, 1990.
- Peeters, P., P. C. Simon, G. Rottman, and T. N. Woods, UARS SOLSTICE data as a calibration and validation for GOME, in *GOME Geophysical Validation Campaign: Final Results and Workshop Proceedings*, edited by P. Fletcher and F. Dodge, *Eur. Space Agency ESA WPP-108*, 75-83, 1996.
- Prag, A. B., and F. A. Morse, Variations in the solar ultraviolet flux from July 13 to August 9, 1968, *J. Geophys. Res.*, **75**, 4613-4621, 1970.
- Prinz, D. K., L. E. Floyd, L. C. Herring, and G. E. Brueckner, On-orbit performance of deuterium calibration lamps during four years of SUSIM operations on the UARS, *Proc. SPIE Int. Soc. Opt. Eng.*, **2831**, 25-35, 1996.
- Reber, C. A., The Upper Atmospheric Research Satellite, *Eos Trans. AGU*, **71**, 1867-1873, 1990.
- Reinsel, G. C., G. C. Tiao, D. J. Wuebbles, J. B. Kerr, A. J. Miller, R. M. Nagatani, L. Bishop, and L. H. Ying, Seasonal trend analysis of published ground-based and TOMS total ozone data through 1991, *J. Geophys. Res.*, **99**, 5449-5464, 1994.
- Rottman, G. J., Observations of solar UV and EUV variability, *Adv. Space Res.*, **8**(7), 53-66, 1988.
- Rottman, G. J., and T. N. Woods, The UARS SOLSTICE, *Proc. SPIE Int. Soc. Opt. Eng.*, **2266**, 317-327, 1994.
- Rottman, G. J., C. A. Barth, R. J. Thomas, G. H. Mount, G. M. Lawrence, D. W. Rusch, R. W. Sanders, G. E. Thomas, and J. London, Solar spectral irradiance, 120 to 190 nm, October 13, 1981, to January 3, 1982, *Geophys. Res. Lett.*, **9**, 587-590, 1982.
- Rottman, G. J., T. N. Woods, and T. P. Sparr, Solar Stellar Irradiance Comparison Experiment: Instrument design and operation, *J. Geophys. Res.*, **98**, 10,667-10,678, 1993.
- Scargle, J. D., Studies in astronomical time series analysis, II, Statistical aspects of spectral analysis of unevenly spaced data, *Astrophys. J.*, **263**, 835-853, 1982.
- Schlesinger, B. M., and R. P. Cebula, Solar variation 1979-1987 estimated from an empirical model for changes with time in the sensitivity of the Solar Backscatter Ultraviolet instrument, *J. Geophys. Res.*, **97**, 10,119-10,134, 1992.
- Schlesinger, B. M., R. P. Cebula, D. F. Heath, M. T. DeLand, and R. D. Hudson, Ten years of solar change as monitored by SBUV and SBUV/2, in *Climate Impact of Solar Variability*, edited by K. H. Schatten and A. Arking, *NASA Conf. Publ.*, CP-3086, 341-348, 1990.
- Schmidtke, G., P. Seidl, and C. Wita, Airglow-solar spectrometer experiment (20-700 nm) aboard the San Marco D/L satellite, *Appl. Opt.*, **24**, 3206-3213, 1983.
- Schmidtke, G., T. N. Woods, J. Worden, G. J. Rottman, H. Doll, C. Wita, and S. C. Solomon, Solar EUV irradiance from the San Marco ASSI: A reference spectrum, *Geophys. Res. Lett.*, **19**, 2175-2178, 1992.
- Simon, P., Solar irradiance between 120 and 400 nm and its variations, *Sol. Phys.*, **74**, 273-291, 1981.

- Smith, E. V. P., and D. M. Gottlieb, Solar flux and its variations, *Space Sci. Rev.*, 16, 771-802, 1974.
- Thullier, G., M. Hersé, P. C. Simon, D. Labs, H. Mandel, and D. Gillotay, Observation of the UV solar spectral irradiance between 200 and 350 nm during the ATLAS 1 mission by the SOLSPEC spectrometer, *Sol. Phys.*, 171, 283-302, 1997.
- Tousey, R., The extreme ultraviolet spectrum of the sun, *Space Sci. Rev.*, 2, 2-69, 1963.
- VanHoosier, M. E., J.-D. F. Bartoe, G. E. Brueckner, and D. K. Prinz, Absolute solar spectral irradiance 120-400 nm (results from the Solar Ultraviolet Spectral Irradiance Monitor-SUSIM-Experiment on board Spacelab 2), *Astrophys. Lett. Commun.*, 27, 163-168, 1988.
- Watari, S., Fractal dimensions of solar activity, *Sol. Phys.*, 158, 365-377, 1995.
- Weber, M., J. P. Burrows, and R. P. Cebula, GOME Solar UV/VIS irradiance measurements in 1995 and 1996 - First results on proxy solar activity studies, *Sol. Phys.*, 177, 63-77, 1998.
- Wehrli, C., C. Fröhlich, and J. Romero, Results of solar spectral irradiance measurements by SOVA2 on EURECA, *Adv. Space Res.*, 16(8), 25-28, 1995.
- Wehrli, Ch., C. Fröhlich, and J. Romero, Space degradation of SOVA sunphotometers on EURECA, *Metrologia*, 32, 653-656, 1996.
- Weiss, H., R. P. Cebula, K. Laamann, and R. D. Hudson, Evaluation of the NOAA 11 solar backscatter ultraviolet radiometer, mod 2 (SBUV/2): Inflight calibration, *Proc. SPIE Int. Soc. Opt. Eng.*, 1493, 80-90, 1991.
- White, O. R., G. J. Rottman, T. N. Woods, B. G. Knapp, S. L. Keil, W. C. Livingston, K. F. Tapping, R. F. Donnelly, and L. C. Puga, Change in the radiative output of the Sun in 1992 and its effect in the thermosphere, *J. Geophys. Res.*, 99, 369-372, 1994.
- Wilson, R. M., On the use of 'first spotless day' as a predictor for sunspot minimum, *Sol. Phys.*, 158, 197-204, 1995.
- Woods, T. N., G. J. Rottman, and G. J. Ucker, Solar Stellar Irradiance Comparison Experiment: Instrument calibration, *J. Geophys. Res.*, 98, 10,679-10,694, 1993.
- Woods, T. N., et al., Validation of the UARS solar ultraviolet irradiances: Comparisons with the ATLAS 1 and 2 measurements, *J. Geophys. Res.*, 101, 9541-9569, 1996.
- Zhou, S., G. J. Rottman, and A. J. Miller, Stratospheric ozone response to short- and intermediate-term variations of solar UV flux, *J. Geophys. Res.*, 102, 9003-9011, 1997.

---

R.P. Cebula and M.T. DeLand (corresponding author), Raytheon STX Corporation, 4400 Forbes Blvd., Lanham, MD 20706 (e-mail:cebula@ssbuvg.sfc.nasa.gov; mdeland@stx.com)

(Received October 8, 1997; revised April 6, 1998; accepted April 7, 1998.)